Production and characterisation of putative early effector proteins in *Chlamydia trachomatis* infection

Jamie Coldwell

Master of Science by Research

University of York

Chemistry

December 2015

Abstract

Chlamydia trachomatis is commonly known as the most common bacterial sexually transmitted infection in the world, having affected approximately 3.1% of the global population in 2010, and being a major cause of infertility in men and women. However, what is less well known among the general population is that *C. trachomatis* also causes the blindness disease trachoma, the leading cause of preventable blindness globally. This project aimed to produce and investigate three proteins known to be involved in the early stages of the infection process: CT694, CT166 and PmpD. CT694 and CT166 are believed to affect actin fibre formation and breakdown, acting in concert with one another to facilitate engulfment of the bacterium by the host. PmpD is a protein which draws significant interest as a vaccination target, as it is present on the outer membrane of *C. trachomatis* and is conserved very highly among serovars.

This project focussed mainly on the breakdown product ΔCT694. Its gene was amplified from Chlamydial genomic DNA and inserted into a plasmid, which was used to transform an expression strain of *Escherichia coli*. Batches of protein were produced for characterisation and investigation, mainly commercial and customised crystallisation screens. Although no crystals were achieved, a promising microcrystalline precipitate formed, and a “best condition” has been recorded. In addition, the fragment PmpD F2 was produced regularly for vaccine studies by inclusion body preparation, and characterisation experiments were performed upon the protein. Work on PCR and gene cloning of PmpD fragments and CT166 was performed as well. Although the primary goal of producing X-ray diffractable crystals was not met, this project has laid the foundations within the group for development and future work.

Contents

Abstract **2**

List of figures **6**

List of tables **11**

Acknowledgements **12**

Author's Declaration **13**

1.0 – Introduction **14**

1.1 – *Chlamydia trachomatis* – background **14**

1.2 – *Chlamydia trachomatis* – infection **15**

1.3 – Chlamydial diseases and impact – trachoma **16**

1.4 – Chlamydial diseases and impact – the STI **17**

1.5 – CT694 – function and interaction **18**

1.6 – CT694 – Previous work: break-down fragment **18**

1.7 – CT166 – Putative function and relationship with CT694 **19**

1.8 – PmpD – Features and putative function **20**

1.9 – Project aims **22**

2.0 – Materials and methods **23**

2.1 – Materials **23**

2.2 – Formulations **24**

2.3 – SDS-PAGE **26**

2.4 – Native gel electrophoresis **27**

2.5 – Agarose gel electrophoresis **27**

2.6 – Polymerase chain reaction (PCR) **27**

2.7 – Gel extraction **28**

2.8 – Restriction enzyme digestion **29**

2.9 – Ligation **29**

2.10 – Transformation and colony PCR **30**

2.11 – Small scale expression test **31**

2.12 – Large scale expression **31**

2.13 – Purification protocol (CT694) **32**

2.14 – Carboxymethylation **33**

2.15 – Inclusion body prep - denaturation and refolding (PmpD F2) **33**

2.16 – Crystallisation **34**

2.17 – Commercial and custom crystal screen list **34**

2.18 – Custom screen maps **36**

3.0 – Results **42**

3.1 – PCR and gene cloning **42**

3.1.1 – ΔCT694 **42**

3.1.2 – CT166 **44**

3.2 – Expression and purification **45**

3.2.1 – ΔCT694 **45**

3.2.2 – CT166 **52**

3.2.3 – PmpD F2 **55**

3.3 – Experiment results **58**

3.3.1 - ΔCT694 **58**

3.3.2 – PmpD F2 **59**

4.0 – Discussion **64**

4.1 – Purification and experimentation **64**

4.2 – Crystal screens **66**

4.3 – PmpD F2 characterisation experiments **68**

5.0 – Future work **69**

5.1 - ΔCT694 and CT166 **69**

5.2 – PmpD **70**

References **71**

List of figures

Figure 1: Diagram of the life cycle of *Chlamydia trachomatis*, from EB invasion to host cell lysis[4]. **15**

Figure 2: Case rates of *C. trachomatis* (blue) in woman aged 15-39 years, contrasted against case rates for pelvic inflammatory disease (red) in women aged 14-44, in British Columbia, Canada from 1994 to 2009[22]. **17**

Figure 3: Comparison of CT694 protein left at 4 °C for different times[26]. The "fresh" sample was of protein purified in the same week. The strong band in the sample left for 4 months was sent for analysis by mass spectrometry. **19**

Figure 4: Diagram showing the post-translational fragments of PmpD, assigned with F-numbers for use in this report[30]. Numbers shown above the fragments are amino acid numbers in the protein sequence. **21**

Figure 5: Crystal screen Custom A, with a pH gradient increasing from rows A to D, three additives and testing of CT694 at concentrations of 40 and 80 mg/ml. **37**

Figure 6: Crystal screen Custom B, with a pH gradient increasing from rows A to D, three different additives compared to Custom A, and testing of CT694 at concentrations of 40 and 80 mg/ml. *wells contain 0.1 M sodium cacodylate (pH 6.5) + 2 M $(NH_4)_2SO_4$, †wells contain 0.1 M Tris (pH 8.5) + 2M $(NH_4)_2SO_4$. **38**

Figure 7: Crystal screen Custom α, using 30 mg/ml ΔCT694. A = 0.1% (w/v) octyl -D-glucopyranoside, B = 10 mM LDAO, C = 5 mM SB-12, D = 1:200 C_8E_5 **38**

Figure 8: Crystal screen Custom β, using 30 mg/ml ΔCT694. E = 0.2 M TMAO, F = 0.1 M NDSB 201, G = 1:333 Brij-30, H = 1:10 C12 POC **39**

Figure 9: Crystal screen Custom γ, using 6 mg/ml ΔCT694. A = 0.017% octyl –D-glucopyranoside, B = 1.67 mM LDAO, C = 0.833 mM SB-12, H = 1:60 C12 POC **39**

Figure 10: Crystal screen Custom δ, using 6 mg/ml ΔCT694. E = 20 mM TMAO, F = 10 mM NDSB 201, G = 2 mM TCEP, H = 5 mM DTT **40**

Figure 11: Crystal screen Custom CM, using 6 and 30 mg/ml carboxymethylated CT694 in separate drops in each well. **40**

Figure 12: Crystal screen Custom X, diluting the mother liquor Index A8 in a gradient from left to right, using 15 and 30 mg/ml CT694 in separate drops in each well. Both carboxymethylated and non-carboxymethylated protein were used, as well as an addition of 10% glycerol. **41**

Figure 13: Successful PCR of ΔCT694. Far left well contained DNA ladder, and the four wells on the right contained PCR product. The arrow indicates the amplified DNA band, as expected at 0.75 kb. **42**

Figure 14: Test to determine whether digestion of pET28b vector was successful. The well on the far left contains DNA ladder. The digested plasmid appears to be at a higher molecular weight than the undigested plasmid. **43**

Figure 15: Successful CPCR of ΔCT694. The left hand wells contained DNA ladder, and the rest all contained PCR product from different colonies. The arrows indicate where the 0.75 kb amplified band was expected to appear, as it did in samples from most colonies. **44**

Figure 16: Successful CPCR of CT166. The left hand wells contained DNA ladder, and the wells on the right all contained PCR product from different colonies. The arrows indicate where the 1.5 kb amplified band was expected to appear, as it did in samples from most colonies. **45**

Figure 17: Small-scale expression test of ΔCT694. A minus sign indicates uninduced cells, a plus sign indicates induced cells. ΔCT694's molecular weight is labelled with an arrow (30 kDa). **46**

Figure 18: Example 1 of 2 of a Ni column UV trace for ΔCT694 (6th Nov 2014). The green gradient line indicates the increasing imidazole concentration. The red and blue UV traces show a peak of protein eluting from the column as this happens (mostly eluting into fractions D14 and D13). **46**

Figure 19: Example 1 of 2 of a size exclusion UV trace for ΔCT694 (6th Nov '14), using a S75 16/60 Superdex column. The blue peaks indicate protein eluting off the column. **47**

Figure 20: Corresponding SDS-PAGE gel of the 6th Nov '14 purification, showing pure ΔCT694 as the final product (D1-E15). SN = supernatant, Pellet = lysate pellet, FT = Ni flowthrough. D14, D13, and D12-8 are all nickel column fractions, C9-12 and D1-E15 are size exclusion fractions. **48**

Figure 21: Example 2 of 2 of a Ni column UV trace for ΔCT694 (15th Jan 2015). The trace shows protein eluting in a relatively sharp peak into fractions D14 and D13. **48**

Figure 22: Example 2 of 2 of a size exclusion UV trace for ΔCT694 (15th Jan '15), using a S75 16/60 Superdex column. The blue peaks indicate protein eluting off the column. The peaks appear broad due to this trace being zoomed in to focus on the peaks and show fractions clearly. **49**

Figure 23: Corresponding SDS-PAGE gel of the 15th Jan '15 purification, showing pure ΔCT694 as the final product. Wash = a sample taken after washing the column post-protein loading, Ni pool = fractions to be loaded onto size exclusion pooled together. D9+8 and D1 are nickel column fractions, C15-D12 and E1-E7 are SEC fractions. **50**

Figure 24: Native gel comparison between size exclusion fractions from the 15th Jan '15 purification. Fractions E1-7 appear to contain mostly monomeric protein, whereas C15-D12 appear to contain mostly oligomer. **50**

Figure 25: Ni column UV trace of carboxymethylated ΔCT694 being eluted after the process (25th Jun ’15). The large signal from 2 to 8 ml is caused by iodoacetic acid being washed from the column before the imidazole gradient (the green line) was started. **51**

Figure 26: SDS-PAGE gel to determine how much ΔCT694 was lost during the process (result: little). Pre-CM = protein before the carboxymethylation process, FT+W = flowthrough and initial column wash pooled together. **51**

Figure 27: Small-scale expression test of CT166. A minus sign denotes uninduced cells, a plus sign denotes induced cells. **52**

Figure 28: Ni column UV trace for CT166 (11th Sep ’14). The blue line shows a peak in signal as protein elutes from the column. **53**

Figure 29: Corresponding SDS-PAGE gel of the 11th Sep ‘14 purification, showing pure, but dilute CT166 as the final product. SN 4 °C = supernatant stored in the fridge over four nights and then tested. SN 20 °C = the same but at room temperature. **54**

Figure 30: Native gel appearing to show that CT166 eluted from the Ni column is almost entirely oligomeric or aggregated. **54**

Figure 31: Example of a Ni column UV trace for PmpD F2 (23rd Jan '15). The peak is noticably broader compared to typical ΔCT694 UV traces. **55**

Figure 32: Example 1 of 2 of a size exclusion UV trace for PmpD F2 (23 Jan '15), using a S200 16/60 Superdex column. The blue peaks indicate protein eluting off the column. The peaks merge noticeably with some intermediate material eluting from the column. **56**

Figure 33: Corresponding SDS-PAGE gel of the 23rd Jan '15 purification, showing pure PmpD F2 as the final product. B12+11 and Ni pool are nickel fractions, the other three (wells 6-8) are SEC fractions. **56**

Figure 34: Native gel showing the different oligomeric states of PmpD F2 eluting from the size exclusion column: OLIG (D9-D1), INT (E2-11) and MON (E13-F12). ALL is a mix of the three. **57**

Figure 35: Example 2 of 2 of a size exclusion UV trace for PmpD F2 (17th Apr '15), using a S200 16/60 Superdex column. **57**

Figure 36: Native gel of the 17th Apr '15 purification showing the different oligomeric states of PmpD F2 eluting from the size exclusion column. **57**

Figure 37: The best condition achieved from crystallisation trials over the course of this project. **58**

Figure 38: A zoomed view of the microcrystalline structure in the crystal drop. **59**

Figure 39: Native gel showing the effect of high and low concentrations of reducing agents on monomeric PmpD F2. **60**

Figure 40: Native gel showing the effect of high and low concentrations of reducing agents on oligomeric PmpD F2. **60**

Figure 41: SDS-PAGE gel showing the effect of different pH levels on monomeric PmpD F2. **60**

Figure 42: SDS-PAGE gel showing the effect of different pH levels on oligomeric PmpD F2. **61**

Figure 43: First attempt at proteolysis of PmpD F2 monomer (gel 1) and oligomer (gel 2) with trypsin and subtilisin. **61**

Figure 44: Second attempt at a proteolysis experiment for monomeric PmpD F2. **62**

Figure 45: Second attempt at a proteolysis experiment with oligomeric PmpD F2. **63**

Figure 46: Mechanism for disulfide bonding. In the case of intra- or intermolecular protein bonds, the R groups are cysteine residues on the same or different proteins. **64**

Figure 47: Mechanism of carboxymethylation of cysteine residues in proteins using iodoacetic acid[32]. **65**

List of tables

Table 1: Materials and pieces of equipment used in this project, and their suppliers. **20**

Acknowledgements

I would like to thank my supervisors Marek Brzozowski and Wayne Paes for all their support, guidance and understanding throughout not only this project but also my BSc work.

I would also like to thank my mother Ruth for helping me fund this project, and to everyone in YSBL for being open to advise or help me whenever I needed it, in particular Simon Grist, Sally Lewis, Shirley Roberts and Sophie McKenna.

Author’s Declaration

I, Jamie Coldwell, declare that this thesis is a presentation of original work, and that I am the sole author. This work has not previously been presented for an award at this, or any other, University. All sources are acknowledged as references.

1.0 - Introduction

1.1 - *Chlamydia trachomatis* - Background

Chlamydia trachomatis is an obligate intracellular parasitic bacteria. The *Chlamydia* genus contains three species: *trachomatis*, *suis* and *muridarum*, which specifically infect humans, pigs, and mice and hamsters respectively. *C. trachomatis* mainly infects human epithelial cells of either the genital tract (of both sexes) or the conjunctiva, although certain serovars can also infect the lymphatic system. Infection of the genital tract causes the most common STI in the developed world, which has been a well-known public health issue for many years. Conjunctiva infection from *C. trachomatis* is predominantly a problem in developing countries, where repeated infection causing inflammatory damage leads to trachoma, a neglected tropical disease which is the most common preventable blindness disease in the world.

The life cycle of *C. trachomatis* is biphasic and complex (Figure 1). Infection begins when a Chlamydial elementary body (EB) attempts to invade a host epithelial cell. Elementary bodies are the invasive form of *C. trachomatis* which the body "sees", and are metabolically inactive[1], similar to a spore. Once the EB is inside the host cell surrounded by an inclusion, it begins transitioning into a reticular body (RB), which is the metabolically active form of *C. trachomatis*. While in this form it divides by binary fission and secretes many proteins which enable the bacteria to survive in the Chlamydial inclusion. It evades processing by the host cell by preventing fusion of the inclusion with phagolysosomal components[2], and localises in the perinuclear region near the Golgi apparatus and endoplasmic reticulum, sequestering nutrients such as sphingolipids and cholesterol from the exocytic pathway[3]. As the number of RBs in the inclusion increase exponentially, it increases in size to take up the majority of the cell volume. In the late stages of intracellular life, RBs begin transitioning into EBs, and are eventually released by cell lysis, or inclusion extrusion. They are then free to infect other cells.

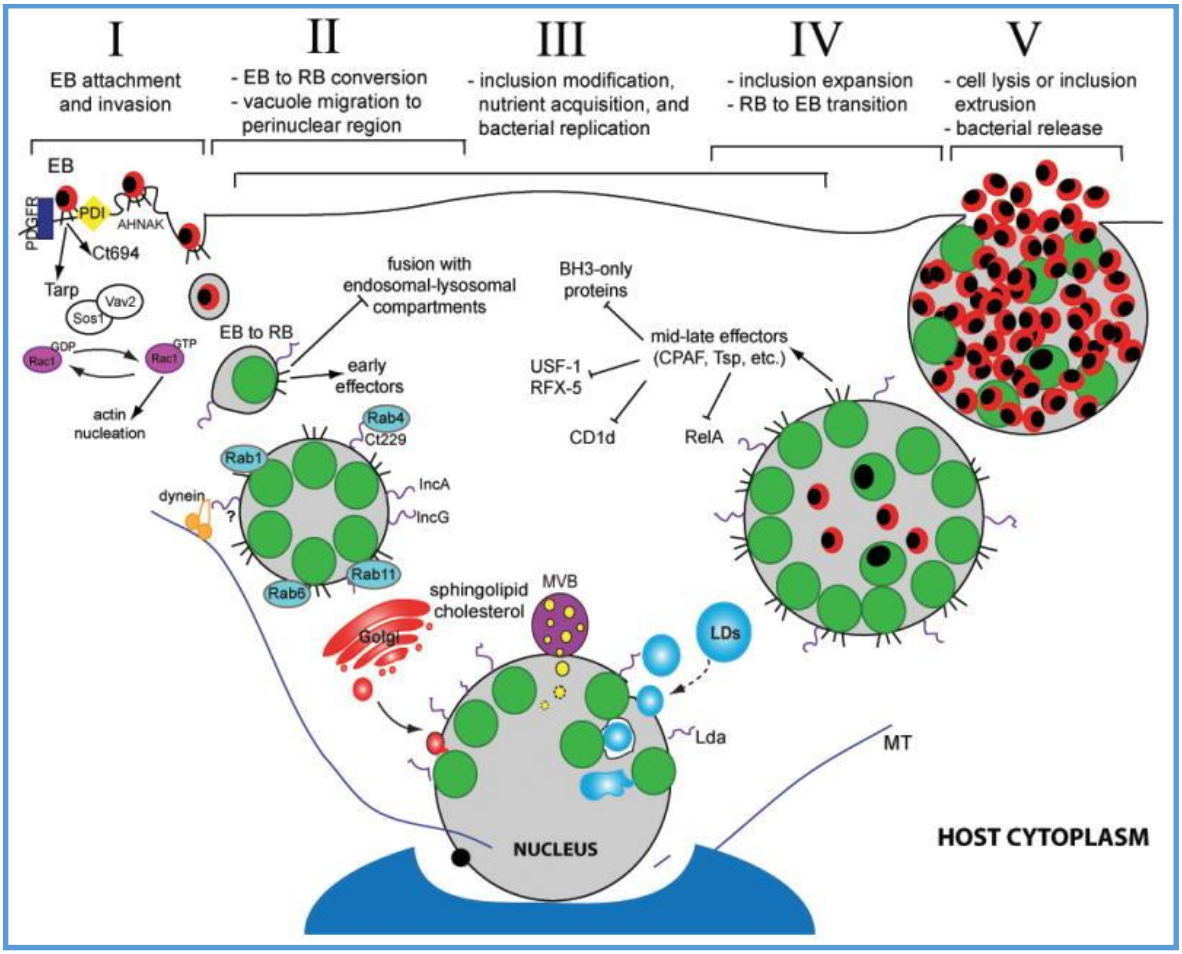

Figure 48: Diagram of the life cycle of *Chlamydia trachomatis*, from EB invasion to host cell lysis[4].

1.2 - *Chlamydia trachomatis* – infection

The aim of *C. trachomatis* is to enter a host cell in order to be able to replicate and expand. Chlamydial EBs attach to a potential host epithelial cell via external adhesins on the outer membrane. They then facilitate their own engulfment by the host[5] by employing a type-III secretion system (T3SS). Once contact with the host has been achieved, effectors of this system such as Tarp and CT694 are secreted in a matter of minutes[6]. These effector toxins affect the host's cytoskeleton, manipulating actin and host cell proteins involved in the organisation of cell shape. The cytoskeleton is reorganised in such a way that it wraps around the EB and engulfs it in an inclusion.

The invasion process of Chlamydia is not well-researched and only a few T3SS effectors in early invasion are known and established. The most well-characterised effector is Tarp (CT456)[7], which is involved in nucleation of actin as preparation for fibre elongation, and is able to recruit actin monomers[8] and cooperate with proteins such as Arp2/3[9]. A class of effectors called the Inc

class handle multiple processes including the ability to intercept materials by affecting membrane trafficking[10], homotypic fusion of inclusions[11], and localisation to the peri-nuclear region. They are membrane-associated with a distinctive bilobed hydrophobic domain, and anchor other proteins in the inclusion membrane. *C. trachomatis* also produces multiple chaperone proteins to aid secretion and translocation of T3SS substrates, often by direct interaction with the secretion assembly; for example the chaperone Slc1 is complexed with CT694 in Chlamydial EBs, and has been shown to interact with Tarp and enhance its secretion[7]. Chaperones have multiple other uses such as offering protection from substrate degradation and preventing effectors from interacting with substrates until necessary.

1.3 - Chlamydial diseases and impact - trachoma

C. trachomatis is the leading cause of preventable blindness in the world[12], as serovars A-C cause trachoma, an infectious eye disease classed as a neglected tropical disease. It is prevalent in developing nations as it thrives in areas with poor general hygiene and lack of access to clean water, among other factors. In 2008 is was estimated that around 60 million people were infected with trachoma[13] over 50 countries, with up to 8 million permanently blind[14] as a result of chronic infection.

Trachoma is infectious, with uninfected individuals able to contract the disease by contact with either secretions from the eyes or nose of an infected person, or more subtlely by contact with a disease vector such as a fly which has touched such a secretion. Disease occurs three times more often in women than men, mainly due to the fact that children are more susceptible to infection and (in developing countries) women come into contact with children more often in general[15]. The primary infection of epithelial cells in the conjunctiva causes roughening of the inside of the eyelids due to inflammation damage, and repeated infection over the course of months or years cause severe scarring on the inside surface of the eyelids. This can cause entropion, where the victim's eyelids turn inwards and the eyelashes scratch the cornea repeatedly, causing permanent, painful blindness.

1.4 - Chlamydial diseases and impact – the STI

Chlamydia is infamous in the western world for being the most common sexually transmitted disease in most developed countries[16], but is also extremely common in developing countries. In 2001 the World Health Organisation (WHO) estimated an incidence rate of 92 million sexually transmitted infections per year[17], the majority of which occur in developing countries due to poor disease control and poor general hygiene. Despite a major focus on *Chlamydia* in public control programs for years, this number is on the rise; in 2010, sexually transmitted *Chlamydia* infections affected 215 million people[18], and 1,200 cases resulted in death[19]. In the province of British Columbia in Canada, which has maintained its *Chlamydia* control program for over 20 years, pelvic inflammatory disease rates have decreased by over 80%, but the number of cases has actually increased by around 50% since the beginning of the program[20] (Figure 2). The main theory as to why this is the case is because treatment is being given to patients too early to establish immune responses which would protect the patient against subsequent reinfection, and hence inhibiting formation of herd immunity, a concept known as the arrested immunity hypothesis[21]. The serovars of *C. trachomatis* which cause genital diseases are serovars D-K. Serovars L1-3 cause lymphogranuloma venereum (LGV), a lymphatic infection associated with HIV co-infection.

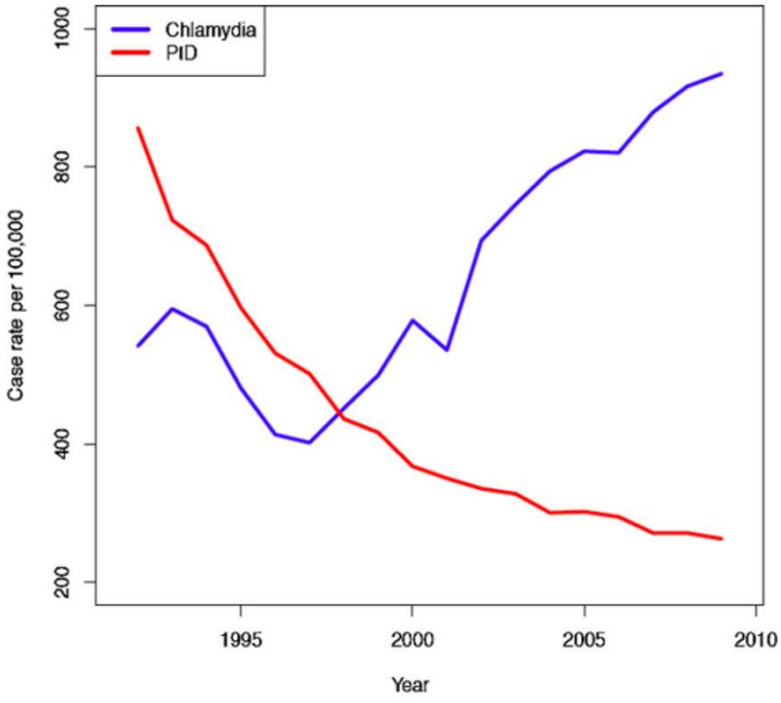

Figure 49: Case rates of *C. trachomatis* (blue) in woman aged 15-39 years, contrasted against case rates for pelvic inflammatory disease (red) in women aged 14-44, in British Columbia, Canada from 1994 to 2009[22].

A sexually transmitted infection involves *Chlamydia* invading epithelial cells of the genital tract; either the urethra of the penis (urethritis), or the cervix (cervicitis). In the case of the male sex, if the infection is left untreated, it can spread to the testicles causing epididymitis, which, if left further, can cause partial or total infertility. The timeframe for infertility to occur is usually 6-8 weeks after contraction. In the case of the female sex, cervicitis is asymptomatic in over 50% of cases, making it difficult to self-diagnose. If undetected, the infection can develop into PID via spread of the infection to the uterus, fallopian tubes and/or ovaries. Symptoms include chronic pain, and the disease can lead to infertility or serious complications with pregnancy including ectopic pregnancy.

1.5 - CT694 – function and interaction

CT694 is a 35 kDa (322 aa) T3SS effector toxin secreted by *C. trachomatis* during early infection. Given that the Chlamydial elementary body is lacking in metabolic activity, it is theorised that early effectors like CT694 are produced and built up during late-cycle activity in reticular bodies, before RB to EB transition[23]; it has been shown that EBs possess a substantial pool of CT694[24]. It contains multiple functional domains, including one domain from residues 40-80 which localises the protein to membranes[25], facilitating targeting of host cell membranes, and a C-terminal domain which interacts with the human protein Ahnak (also known as desmoyokin) which has downstream effects on cell morphology; CT694 specifically interacts with the central repeat-unit domain and the C-terminal domain of Ahnak, and in doing so affects the actin cytoskeleton and stress fibres[24]. CT694 also has Ahnak-independent effects on cell morphology. The direct consequences of CT694 action in terms of pathways and proteins affected are unclear.

1.6 - CT694 – Previous work: break-down fragment

Work was first started on CT694 in the Brzozowski group at York Structural Biology Laboratory in 2013. The CT694 gene was amplified from *C. trachomatis* genomic material using polymerase chain reaction (PCR) with specific primers, cloned, and used to transform expression strains of *Escherichia coli*. CT694 purified relatively easily using Ni-affinity chromatography followed by gel filtration, producing a high yield. However the protein was unstable, consistently producing what appeared to be multiple breakdown bands in SDS poly-acrylamide gel electrophoresis (SDS-PAGE) gels, even

when fresh from purification. This is not ideal for crystallisation prospects or other characterisation experiments.

CT694 protein was left at 4 °C for 4 months as a study to determine if it formed a stable breakdown product. Protein was compared on an SDS-PAGE gel at a few timepoints from the 4 month period (Figure 3). There appeared to be a stable fragment at about 30 kDa termed ΔCT694, with the breakdown bands at such low molecular weights that they ran off the gel. The band was excised from the gel and sent for sequencing by mass spectrometry (MS). Using the sequence results, the breakdown fragment (ΔCT694)'s gene will be copied, cloned and used to transform expression strains in an attempt to produce the protein and characterise it, hopefully developing crystals in order to determine a crystal structure.

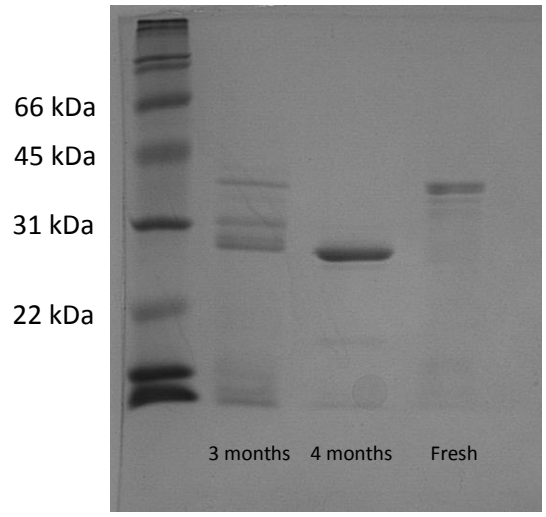

Figure 50: Comparison of CT694 protein left at 4 °C for different times[26]. The "fresh" sample was of protein purified in the same week. The strong band in the sample left for 4 months was sent for analysis by mass spectrometry.

1.7 - CT166 – Putative function and relationship with CT694

CT166 is a 72 kDa Chlamydial toxin and is also active early in the *C. trachomatis* infection process. Although it has not been shown that it is a T3SS effector, it is thought that this is the case. Interestingly, CT166's effect on the host cell's morphology is very different to that of CT694. CT694 seems to induce nucleation and elongation of actin filaments, while CT166 induces rounding of the cell shape and a decrease in cell diameter[27]. Thus, it is theorised that the two proteins work in concert with one another, with CT694 causing the cell to extend its membrane around the Chlamydial EB, and CT166 causing the actin filaments and membrane to shrink and pull the EB into the host cell, engulfed in an inclusion.

Sequence alignment studies have shown that CT166 shows significant homology with glucosylating toxins from the *Clostridia* genus, specifically their glucosyltransferase domain near the N-terminus. Both clostridial toxins and CT166 contain an important DXD motif[28], which clostridial toxins utilise to add glucosyl groups to GTP-binding proteins of the Rho and Ras families, otherwise known as "the master regulators of the actin cytoskeleton". Although CT166 also targets a Rho-family GTPases Rac and CDC42, the DXD motif is not essential for CT166's activity on actin reorganisation. It has recently been found that this motif is instead involved in ERK and PI3K inhibition, resulting in delay of progression of the host cell cycle. This shows that CT166 is a multifunctional protein which plays an important role in Chlamydial invasion and survival.

1.8 - PmpD – Features and putative function

Polymorphic membrane protein D, or PmpD, is a *C. trachomatis* protein localised to the exterior of the outside membrane of the EB. Its native form is oligomeric with an interesting pore-like structure 23 nm in diameter[29], with each monomer similar in appearance to a flower petal circling the pore in the middle; full-length PmpD (about 155 kDa) is present as well as two proteolysed fragments, the passenger domain fragment (~73 kDa) and a beta-barrel translocator domain (~82 kDa). In other studies, it has been shown that the full passenger domain is actually around 120 kDa, with the translocator domain being around 35 kDa[30]; Figure 4 maps the fragments of PmpD. While on the exterior of the bacterium, it is theorised to act as an adhesin, forming a bond between the parasite and the host cell membrane. *C. trachomatis* is then in a position to employ its T3SS mechanism to initate invasion. Once inside the cell, PmpD has been shown to undergo further proteolytic processing reaction to yield soluble peptides which contain motifs possibly for interacting with eukaryotic proteins (for example nuclear localisation signals)[29], suggesting that PmpD can have secondary effects on the host cell, or even in neighbouring cells.

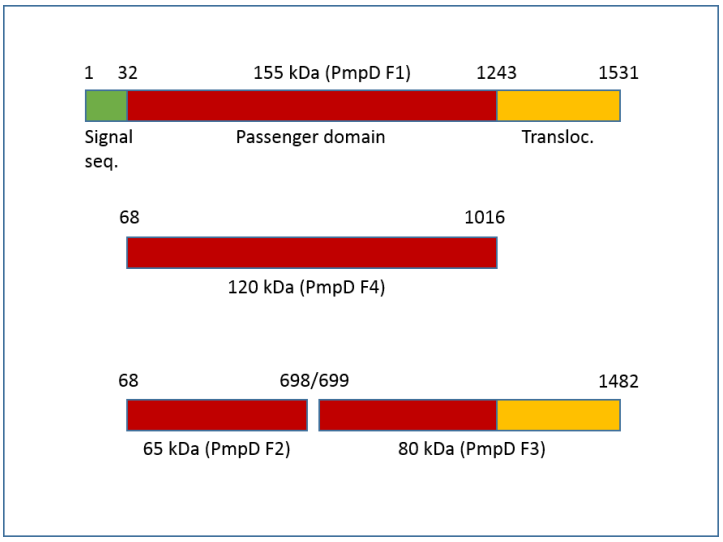

Figure 51: Diagram showing the post-translational fragments of PmpD, assigned with F-numbers for use in this report[30]. Numbers shown above the fragments are amino acid numbers in the protein sequence.

Current treatment plans for *C. trachomatis* have decreased the incidence of disease, but case rates are rising, possibly due to lack of opportunity for immunity development. A vaccine is the ideal solution to the problem, and has become a feasible one thanks to advancements in genomics and immunology[22]. PmpD is 99% conserved across all *C. trachomatis* serovars and therefore makes for a promising vaccine target. In vitro, it has been shown that antibodies (Ab) specific to PmpD are able to neutralise *C. trachomatis*[31]. However, Ab against more common targets on the cell membrane and which are serovariable, the best example of which being major outer membrane protein (MOMP), block the neutralisation of PmpD. This points towards an immune evasion strategy in vivo in which antigens specific to certain serovars, or even polymorphic antigens, are common/immunodominant on the bacterial exterior, and block access to PmpD and hence block neutralisation. This could be a contributing factor as to why immunity takes a long time to manifest from natural infection. In this case, in terms of vaccine strategy it seems necessary to use recombinant PmpD as the vaccine agent rather than an attenuated form of *C. trachomatis*, in order to protect against all serovars of the bacterium.

1.9 - Project aims

The primary aims of this project were:

- To isolate and copy the ΔCT694 gene from either frozen CT694 DNA from previous cloning, or from *C. trachomatis* genomic material, and clone it in order to transform expression strains
- To use these *E. coli* expression strains to produce the protein for purification, and to observe any difference in stability compared to full-length CT694
- To attempt crystallisation screens and optimisation on ΔCT694 in order to solve a novel crystal structure
- To regularly produce PmpD F2 for vaccine studies

Secondary aims:

- To isolate and copy the CT166 gene from *C. trachomatis* genomic material, clone it, and transform expression strains of *E. coli*
- To use these expression strains to produce the protein for purification
- To attempt crystallisation trials on CT166 and PmpD fragments
- To isolate genes in order to clone and produce different fragments of PmpD (F1, F3 and F4)
- To characterise the different PmpD fragments and compare the results with those from PmpD F2

2.0 - Materials and methods

2.1 - Materials

Category	Material	Supplier
Chemical	Tris hydrochloride (Tris)	Sigma
	Sodium chloride (NaCl)	VWR Chemical
	Dithiothreitol (DTT)	Melford
	Tryptone	Lab M
	Yeast extract	Lab M
	Agar No. 1	Lab M
	Isopropyl β-D-1-thiogalactopyranoside (IPTG)	Sigma
	Kanamycin	ThermoFisher Scientific
	Guanidinium hydrochloride	Sigma
	Imidazole	Sigma
	SigmaFAST EDTA-free protease inhibitor tablets	Sigma
	Iodoacetic acid	Sigma
	Reduced glutathione	Sigma
	Poly(ethylene glycol) (PEG) 550 monomethyl ether (MME)	Sigma
	PEG 3350	Sigma
	PEG 8000	Sigma
	Dioxane	Sigma
	L-proline	Sigma
	Lauryldimethylamine *N*-oxide (LDAO)	Sigma
	Sulfobetaine 12 (SB-12)	Sigma
	Pentaethylene glycol monooctyl ether (C_8E_5)	Sigma
	Polyoxyethylene(4)lauryl ether (Brij 30)	Sigma
	3-(1-pyridinio)-1-propanesulfonate (NDSB 201)	Calbiochem
	Octyl β-D-glucopyranoside	Calbiochem
	Maltose	Melford
	Glucose	Fisher
	Ammonium sulfate	Fisher

	Glycerol	Fisher
	Sodium acetate	Fisher
	Bond Breaker TCEP solution	Thermo Scientific
	Trimethylamine *N*-oxide (TMAO)	Fluka Analytical
	Mercury chloride	Sigma
	Antarctic shrimp phosphatase	New England Biolabs
Equipment	5ml HisTrap Ni-Sepharose column	GE Healthcare
	ÄKTA Explorer	GE Healthcare
	Amicon Ultra centrifugal filter units	Millipore
	RC-5B Plus centrifuge	Sorvall
	Hydra II	Matrix Tech
	Mosquito Crystal	TTP Labtech
	Innova 44 Shaker	Eppendorf
	INGENIUS gel photography system	SynGene
	BioPhotometer (spectrophotometer)	Eppendorf
	ND-1000 Spectrophotometer	NanoDrop
	LifeEco thermocycler	BIOER

Table 1: Materials and pieces of equipment used in this project, and their suppliers.

2.2 - Formulations

Liquid broth (LB) and LB agar, per 1 L:

- 10 g tryptone
- 10 g NaCl
- 5 g yeast extract
- For agar: 16 g Agar No. 1

SDS-PAGE sample buffer (4x):

- 120 mM Tris, pH 6.8
- 20% glycerol (v/v)
- 4% SDS (w/v) (Sigma)
- 1.2 M β-mercaptoethanol
- 10% bromophenol blue (v/v)

Broad range molecular weight ladder for SDS-PAGE (Biorad standard):

- 200 kDa: Myosin
- 116 kDa: β-galactosidase
- 97.4 kDa: Phosphorylase B
- 66.2 kDa: Serum albumin
- 45.0 kDa: Ovalbumin
- 31.0 kDa: Carbonic anhydrase
- 21.5 kDa: Trypsin inhibitor
- 14.4 kDa: Lysozyme
- 6.50 kDa: Aprotinin

1 kilobase (kb) DNA ladder for agarose gel electrophoresis (New England Biolabs):

- 10 kb (84 ng/µl)
- 8.0 kb (84 ng/µl)
- 6.0 kb (100 ng/µl)
- 5.0 kb (84 ng/µl)
- 4.0 kb (66 ng/µl)
- 3.0 kb (250 ng/µl) (reference band)
- 2.0 kb (96 ng/µl)
- 1.5 kb (72 ng/µl)
- 1.0 kb (84 ng/µl)
- 0.5 kb (84 ng/µl)

TAE buffer (1x):

- 40 mM Tris, pH 8.0
- 20 mM Acetic acid
- 5 mM EDTA

2.3 - SDS-PAGE

Recipe for a 12% SDS-PAGE resolving gel:

- 3.2 ml deionised water
- 2.5 ml resolving gel buffer:
    - 1.5 M Tris (pH 8.8)
    - 0.4% SDS
- 4.2 ml acrylamide (Sigma)
- 50 µl ammonium persulfate (APS) (Sigma)
- 8 µl tetramethylethylenediamine (TEMED) (Sigma)

The resolving gel was poured into a gel caster, topped with 1 ml butan-1-ol and left to set. Then a stacking gel was poured on top:

- 3.2 ml deionised water
- 1.3 ml stacking gel buffer:
    - 0.5 M Tris (pH 6.8)
    - 0.4% SDS
- 0.5 ml acrylamide
- 25 µl APS
- 8 µl TEMED

Once samples were loaded, gels were run at 200 V for 55 min.

SDS-PAGE running buffer:

- 25 mM Tris
- 192 mM glycine (Sigma)
- 0.1% SDS

2.4 – Native gel electrophoresis

Recipe for a 7.5% native gel:

- 4.9 ml deionised water
- 2.5 ml resolving gel buffer
- 2.5 ml acrylamide
- 50 µl APS
- 8 µl TEMED

Once samples were loaded, gels were run at 100 V for 120 min.

Native running buffer:

- 25 mM Tris
- 192 mM glycine

2.5 – Agarose gel electrophoresis

To make an agarose gel, 0.7 g agarose powder (Sigma) was added to 70 ml TAE (Tris, acetic acid and EDTA) buffer and heated in a microwave at full power for 1.5 min. Once the gel had cooled until the flask was able to be held in one's hand, 1 µl SYBR Safe DNA stain (Life Tech.) was added. The mix was poured into a gel holder prepared with masking tape, and a gel comb was added. The gel was then allowed to set. Once samples were loaded, gels were run at 110 V for 45 min. The running buffer was TAE buffer.

2.6 - Polymerase chain reaction (PCR)

The 25 µl total PCR recipe consisted of the following:

- 14.5 µl nuclease-free water
- 5 µl polymerase buffer (New England Biolabs (NEB))
- 2 µl template DNA
- 1.25 µl 10 mM 5' forward primer

- 1.25 µl 10 mM 5' reverse primer
- 0.5 µl 10 mM deoxynucleotide triphosphates
- 0.5 µl Q5 DNA polymerase (NEB)

The initial denaturation took place at 98 °C for 30 s. The reaction underwent 30 cycles of: 98 °C for 30 s, 55-75 °C over 30 s, then 72 °C for 200 s. The final extension was at 72 °C for 360 s, and then the reaction was held at 4 °C.

The DNA was run on an agarose gel to check if the PCR was successful.

2.7 - Gel extraction

Gel extraction was performed using a QIAGEN Gel Extraction Kit and by using the following protocol:

- The DNA fragment was excised from the agarose gel with a scalpel.
- The gel slice was weighed and 3 volumes of buffer QG were added to 1 volume of gel (assumed: 100 mg = 100 ml).
- The mixture was incubated at 50 °C and occasionally vortexed until the gel had completely dissolved.
- The colour of the mixture was checked to ensure it was still yellow (pH <7.5). 1 gel volume of isopropanol was added to the sample and mixed.
- A QIAquick spin column was placed in a 2 ml collection tube. The DNA sample was added to the column and centrifuged for 1 min.
- The flowthrough was discarded and the QIAquick column was placed in another, clean collection tube.
- Nuclease-free water was heated to 65 °C and 30 µl was added to the membrane and left at room temperature for 5 min.

The column was centrifuged again and the DNA was collected in the flowthrough.

2.8 - Restriction enzyme digestion

Recipe for 50 µl total pET28(b) vector digest:

- 2 µl pET28(b) vector
- 5 µl 10x restriction enzyme buffer
- 1 µl Antarctic shrimp phosphatase
- 1 µl NcoI (NEB)
- 1 µl XhoI (NEB)
- 40 µl nuclease-free water

Recipe for 40 µl total CT694 fragment:

- 15 µl CT694 fragment
- 4 µl 10x restriction enzyme buffer
- 1 µl NcoI
- 1 µl SalI (NEB)
- 19 µl nuclease-free water

These reactions were left at room temperature overnight to ensure digestion was completed.

2.9 - Ligation

25 µl total ligation recipe:

- 2 µl 10x ligase buffer
- 2 µl 100mM DTT
- 1 µl 10mM adenosine triphosphate (ATP)
- 5 µl vector
- 5 µl insert
- 1 µl T4 DNA ligase (NEB)
- 9 µl nuclease-free water

Two controls were also run: a reaction was run without the insert, and also a reaction was run without the insert or the T4 DNA ligase. These reactions were incubated at 16 °C overnight.

2.10 - Transformation and colony PCR (CPCR)

The plasmids were used to transform NovaBlue GigaSingles competent cells (EMD Millipore). The cells were thawed and mixed gently to ensure even suspension. 1 µl plasmid was added to each tube of cells and the mixture was stirred gently, and then placed on ice for 5 min. The cells were heat-shocked at 42 °C for 30 s in a heating block, and then placed on ice for 2 min. 125 µl of SOC medium (super optimal broth with catabolite repression) was added to each tube and then they were incubated at 37 °C, shaking in a heat block for 60 min. 50 µl of cells from each tube were spread on a plate of selective LB agar medium with added kanamycin and the plates were incubated at 37 °C overnight.

Master mix for CPCR was created by calculating the contents of one PCR tube (minus template DNA) and then multiplying by the number of colonies to be tested. Colonies were picked from the plates and mixed into 20 µl nuclease-free water. Some colony mix was taken in a PCR tube for each colony, and heated at 94 °C for 10 min to lyse the cells and expose the (template) DNA. Master mix was then added to each tube and the reaction was set up. An example of master mix for a 16-colony CPCR:

- 2 µl 10x PCR buffer (32 µl into master mix)
- 0.25 µl Taq polymerase (4 µl into master mix)
- 0.5 µl 10mM dNTPs (8 µl into master mix)
- 1 µl forward primer (16 µl into master mix)
- 1 µl reverse primer (16 µl into master mix)
- 11.25 µl nuclease-free water (180 µl into master mix)

This resulted in 256 µl total master mix for 16 reactions. 16 µl of master mix was added to each 4 µl PCR tube of colony mix making up to a 20 µl reaction volume per tube.

2.11 - Small-scale expression test

For a small-scale expression test, the plasmids were used to transform BL21 Gold strain of *Escherichia coli*. The cells were thawed and mixed gently to ensure even suspension. 1 µl plasmid was added to the cells and the mixture was stirred gently, and then placed on ice for 5 min. The mixture was heat-shocked at 42 °C for 30 s in a heating block, and then placed on ice for 2 min. 125 µl of LB medium was added to the tube and then the cells were incubated at 37 °C, shaking in a heat block for 60 min. The cells were spread on separate plates of selective LB agar medium with added kanamycin, and incubated at 37 °C overnight.

Individual colonies were picked from the plates the next day with a sterile pipette tip, and then the tips were each ejected into 5ml of sterile LB with 50 µg/ml kanamycin. They were then incubated at 37 °C and shaken, and the OD_{600} (optical density at 600 nm-wavelength light) of the cells was measured using a spectrophotometer. The OD_{600} was allowed to increase to 2.0, at which point the cells' production of CT694 was induced by addition of 1mM IPTG (5 µl of 1 M IPTG added). The cells were then incubated at 16 °C, 20 °C or 37 °C overnight.

The cells were spun using a microcentrifuge (Eppendorf) at 1000 *g* for 5 min. The supernatant was discarded and the cell pellets were resuspended in 15 ml 20mM Tris (pH 8.0), and then sonicated for 10 x 1 min with 30 s breaks to lyse the cells. 15 µl of lysate was mixed with 5 µl of 4x SDS-PAGE sample buffer and run on an SDS-PAGE gel to analyse the expression.

2.12 - Large-scale expression

For large-scale expression, the plasmids were used to transform BL21 Gold expression strain of *Escherichia coli*. 25 µl cells were thawed and mixed gently to ensure even suspension. 1 µl plasmid was added to the cells and the mixture was stirred gently, and then placed on ice for 5 min. The mixture was heat-shocked at 42 °C for 30 s in a heating block, and then placed on ice for 2 min. 125 µl of LB medium was added to the tube and then the cells were incubated at 37 °C, shaking in a heat block for 60 min. 50 µl of cells from the tube were spread on a plate of selective LB agar medium with added kanamycin and incubated at 37 °C overnight. The rest of the cells were frozen at -80 °C for later use.

Individual colonies were picked from the plate with a sterile pipette tip, and then the tip was ejected into 20 ml of sterile LB with 50 µg/ml kanamycin to make starter cultures. These starter cultures were incubated at 37 °C and shaken overnight.

The starter cultures were added (without the pipette tip) the next day to bevelled flasks containing 1 L each of sterile LB with 50 µg/ml kanamycin: two starter cultures to one main flask. The flasks were incubated at 37 °C and shaken. The OD_{600} was allowed to increase to 0.6, at which point the cells' production of CT694 was induced by addition of 1mM IPTG (1ml of 1M IPTG added). The flasks were then incubated at 16 °C or 37 °C and shaken.

2.13 - Purification protocol (CT694)

Buffers:

- Ni buffer A: 20 mM Tris (pH 8.0), 50 mM NaCl, 10 mM imidazole
- Resuspension buffer: Ni buffer A + SigmaFAST EDTA-free protease inhibitor tablets
- Ni buffer B: 20 mM Tris (pH 8.0), 50 mM NaCl, 1 M imidazole
- Size exclusion (SEC) buffer: 20 mM Tris (pH 8.0), 50 mM NaCl

The cells were centrifuged at 6000 *g* at 4 °C for 15 min to pellet the cells. The supernatant was poured off, and the cell pellets were resuspended in 20 ml resuspension buffer. The resuspended cells were pooled and sonicated for 20 x 1 min with 30 s breaks, to lyse the cells. The cell lysate was then centrifuged at 17200 *g* to separate insoluble cell debris from the soluble fraction. The supernatant was pooled into a beaker and kept on ice.

A 5 ml HisTrap Ni-Sepharose column was washed with 5 column volumes (CVs) of water, followed by 5 CVs of Ni buffer A to equilibrate it, using a peristaltic pump. The lysate supernatant was recirculated through the column for at least 2 h to allow the His-tagged protein to bind to the column. The column was then connected to an ÄKTA Explorer, pre-pump-washed into Ni buffers A and B. A gradient was then run from 0% to 100% buffer B (10 mM imidazole to 1 M imidazole) over 25 min at 2 ml/min. 4 ml fractions were collected as the gradient was run.

After viewing the chromatogram, appropriate fractions were pooled and kept on ice. A 2 ml loop was washed with five CVs of water, five CVs of ethanol, five CVs of water and finally five CVs of SEC buffer, before being connected to the ÄKTA. The injection system was flushed with more SEC buffer, and a S75 16/60 Superdex size exclusion column (pre-equilibrated in SEC buffer) (100

ml column volume) was also attached to the ÄKTA. The Ni column pool was injected into a loop, and then injected onto the column by running SEC buffer through the loop. The column was allowed to run at 0.5 ml/min for 3 h 30 min. 1 ml fractions were collected during the run. Fractions containing protein were pooled, and samples for analysis were taken (for example, Bradford assay and SDS-PAGE). The protein was then flash-frozen in liquid nitrogen in 1 ml aliquots, and stored at -80 °C.

2.14 - Carboxymethylation

During the project, an optional carboxymethylation step was added to the protocol. This occurred before the nickel column was eluted. The protein was circulated through the column as normal to allow binding, followed by a washing step with Ni buffer A (5 CVs). Then, 50 ml carboxymethylation buffer (20 mM Tris (pH 8.0), 50 mM NaCl, 20 mM iodoacetic acid) was circulated through the column overnight. The column and buffer were wrapped in aluminium foil during the process because iodoacetic acid can photodegrade. The column was then washed with Ni buffer A as normal followed by eluting with buffer B.

2.15 - Inclusion body prep – denaturation and refolding (PmpD F2)

PmpD F2 requires a different protocol to ΔCT694. After large-scale expression in 2 L flasks, the cells were centrifuged at 6000 *g* at 4 °C for 15 min to pellet the cells. The supernatant was poured off, and the cell pellets were resuspended in 30 ml SEC buffer. The cells were pooled and sonicated for 30 x 45 s with 30 s breaks to lyse the cells, and the cell lysate was then centrifuged at 17200 *g*. The supernatant was discarded and the pellets were kept.

The insoluble pellets were suspended in 20 mM Tris (pH 8.0), 6 M guanidinium hydrochloride (GdmHCl) by stirring overnight at 4 °C. The next day, the protein was dialysed into 20 mM Tris (pH 8.0), 3 M GdmHCl using 8-10 kDa dialysis tubing (Spectrum) overnight at 4 °C, and 1 M GdmHCl the next night. The following day, the samples were centrifuged once more at 17200 *g* to pellet out aggregates. A 5 ml HisTrap Ni-Sepharose column was washed with 5 CVs of water followed by 5 CVs of 20 mM Tris (pH 8.0), 1 M GdmHCl, 10 mM imidazole for equilibration.

Imidazole was added to 10 mM to the soluble PmpD F2 supernatant, and then the PmpD F2 was loaded slowly onto the column. Solutions of 0.5 M and 0.25 M GdmHCl were prepared by

mixing 1 M GdmHCl with Ni buffer A. The column with PmpD F2 bound was then washed with 5 CVs of 0.5 M and 0.25 M GdmHCl to refold the protein fully while bound to the column, followed by 5 CVs of Ni buffer A. The purification procedure was similar to CT694 from this point onwards: Ni column elution, size exclusion (S200 column) and flash-freezing.

2.16 - Crystallisation

The purified protein was used in commercially sourced crystal screens, 96-well plates containing a multitude of different buffers. The screens were dispensed from deep-well plates into crystallisation plates using a Hydra II fluid dispensing machine, at 54 µl per well. Protein was then dispensed into each well and mixed with each condition using a Mosquito Crystal liquid handler. The plates were sealed and then placed in a cool room.

Protein was also used to set up hanging drop customised screens. 1ml conditions were prepared in the wells of 24-well cell culture plates (Corning). The rims of each well were then lined with vacuum grease (Corning). Protein and conditions were mixed in a 1:1 ratio on a cover slips (Fisher) which had previously been siliconised using AquaSil fluid (Thermo Scientific), and then the cover slips were turned upside-down and pressed onto each well such that the vacuum grease formed a seal, and the protein-condition mix drop was hanging into the well. These plates were then placed in a cool room.

2.17 - Commercial and custom crystal screen list

ΔCT694 screens:

- 08/11/14:
    - Hampton Index 96-well
    - Molecular Dimensions PACT 96-well
    - Hampton Crystal Screen 1and2 96-well
    - Hampton 2-methyl-2,4-pentandiol (MPD) 96-well
    - Molecular Dimensions poly-γ-glutamic acid (PGA) 96-well
    - Hampton poly-ethylene glycol (PEG) ion 1and2 96-well
- 13/11/14: (“D1-E5” – different SEC fracs)
    - Hampton Index 96-well

- Molecular Dimensions PACT 96-well
- Hampton Crystal Screen 1and2 96-well
- Molecular Dimensions Clear Strategy Screen (CSS) 1and2 96-well

- 23/02/15:
  - Hampton Index 96-well
  - Molecular Dimensions PACT 96-well
- 25/02/15:
  - Hampton detergent screen 96-well
  - Hampton additive screen [Index D5 ML] 96-well
  - Hampton additive screen [Custom 2 ML] 96-well
- 16/04/15
  - Custom A [pH gradient, 80 or 40 mg/ml] 24-well
  - Custom B [pH gradient, 80 or 40 mg/ml] 24-well
- 02/06/15
  - Custom α [Detergents] (30 mg/ml) 24-well
  - Custom β [Detergents] (30 mg/ml) 24-well
- 11/06/15
  - Custom γ [Diluted detergents] (6 mg/ml) 24-well
  - Custom δ [Diluted detergents] (6 mg/ml) 24-well
- 26/06/15
  - Custom carboxymethylation (CM) (30 and 6 mg/ml) 6-well (12 drops)
- 10/07/15
  - Custom X [ML dilutions, ±glycerol, ±CM] (30 or 15 mg/ml) 24-well (48 drops)

CT166 screens:

- 20/09/14:
  - Hampton Index (24 mg/ml) 96-well
  - Molecular Dimensions PACT (24 mg/ml) 96-well
  - Hampton Index (12 mg/ml) 96-well

2.18 – ΔCT694 custom screen maps

Figures 5 to 12 show maps explaining the layout of the custom screens created during the crystallisation trial process on ΔCT694. After primary screening with commercial pre-formulated screens, the most promising conditions were chosen to take forward for secondary, customised screening, as well as two custom conditions. These are:

- PGA screen, well A10 (minus PGA)
    - 0.1 M sodium acetate (NaOAc), pH 5.0
    - 30% PEG 400 (v/v)
- Index screen, well A2
    - 0.1 M NaOAc, pH 4.5
    - 2 M ammonium sulfate ($(NH_4)_2SO_4$)
- Index screen, well A8
    - 0.1 M NaOAc pH 4.5
    - 3 M NaCl
- Index screen, well D5
    - 0.1 M NaOAc pH 4.5
    - 25% PEG 3350 (w/v)
- Custom 1
    - 0.1 M sodium cacodylate (NaCac), pH 6.5
    - 2 M $(NH_4)_2SO_4$
- Custom 2
    - 0.1 M Tris, pH 8.5
    - 2 M $(NH_4)_2SO_4$

Custom A [pH gradient, 80 or 40 mg/ml] 24-well:

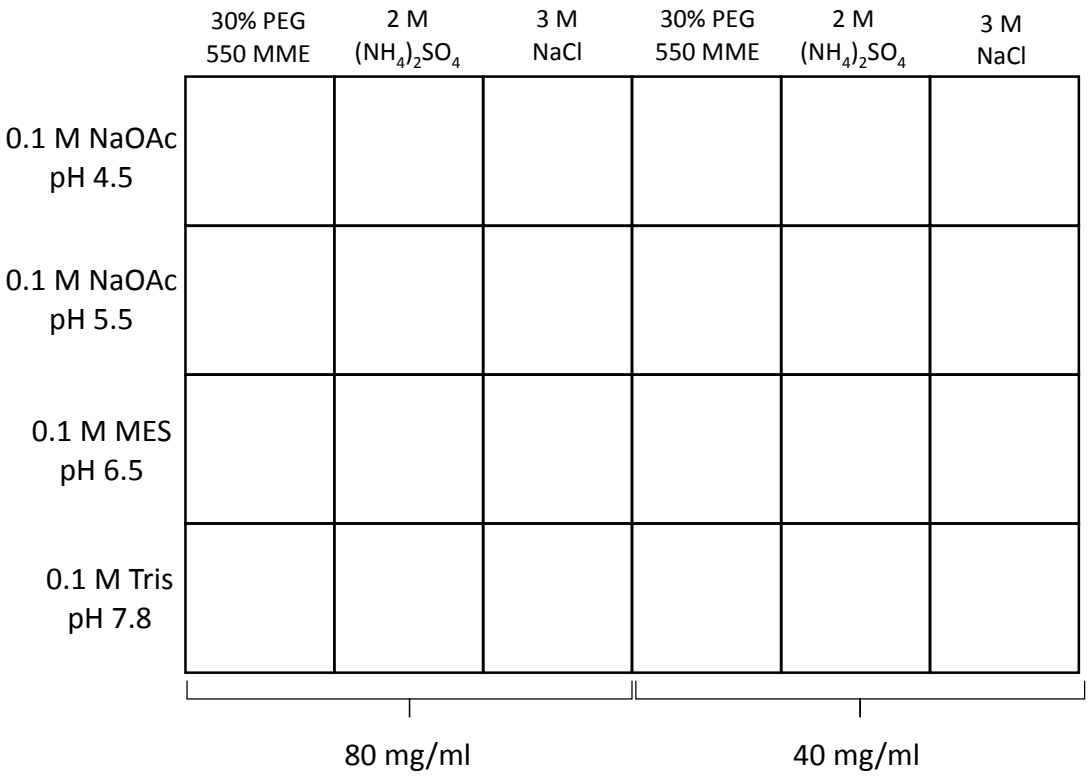

Figure 52: Crystal screen Custom A, with a pH gradient increasing from rows A to D, three additives and testing of CT694 at concentrations of 40 and 80 mg/ml.

16/04/15 - Custom B [pH gradient, 80 or 40 mg/ml] 24-well:

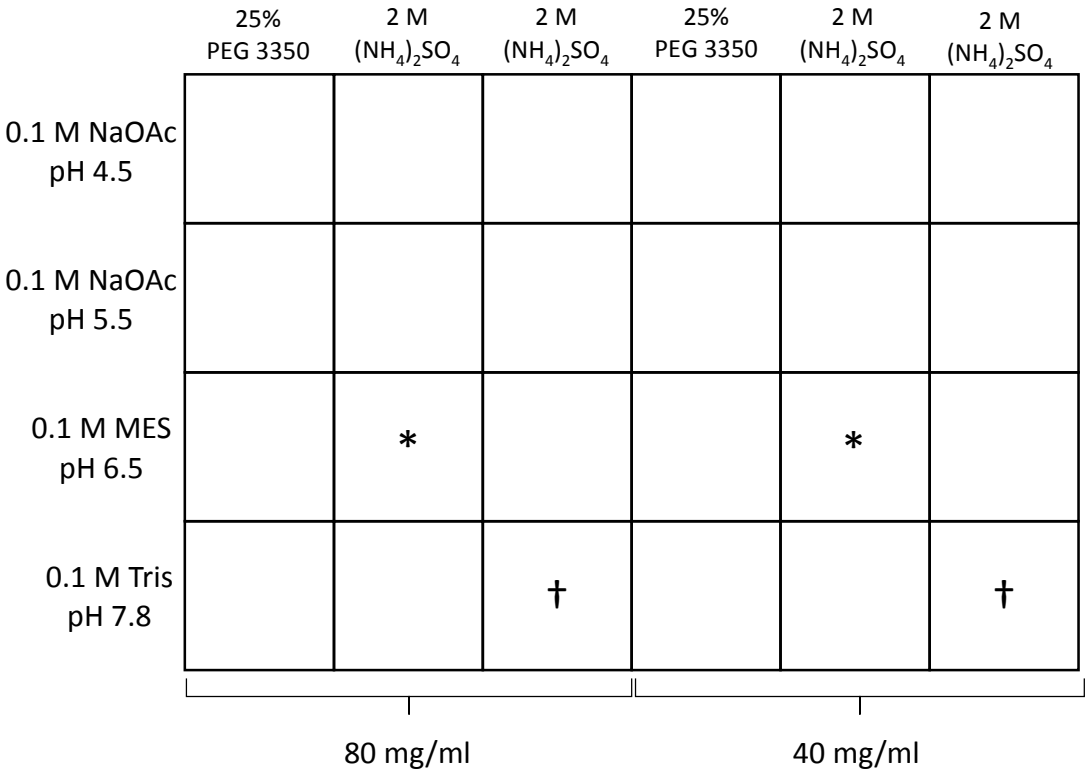

Figure 53: Crystal screen Custom B, with a pH gradient increasing from rows A to D, three different additives compared to Custom A, and testing of CT694 at concentrations of 40 and 80 mg/ml. *wells contain 0.1 M sodium cacodylate (pH 6.5) + 2 M $(NH_4)_2SO_4$, †wells contain 0.1 M Tris (pH 8.5) + 2M $(NH_4)_2SO_4$.

02/06/15 - Custom α [Detergents] (30 mg/ml) 24-well:

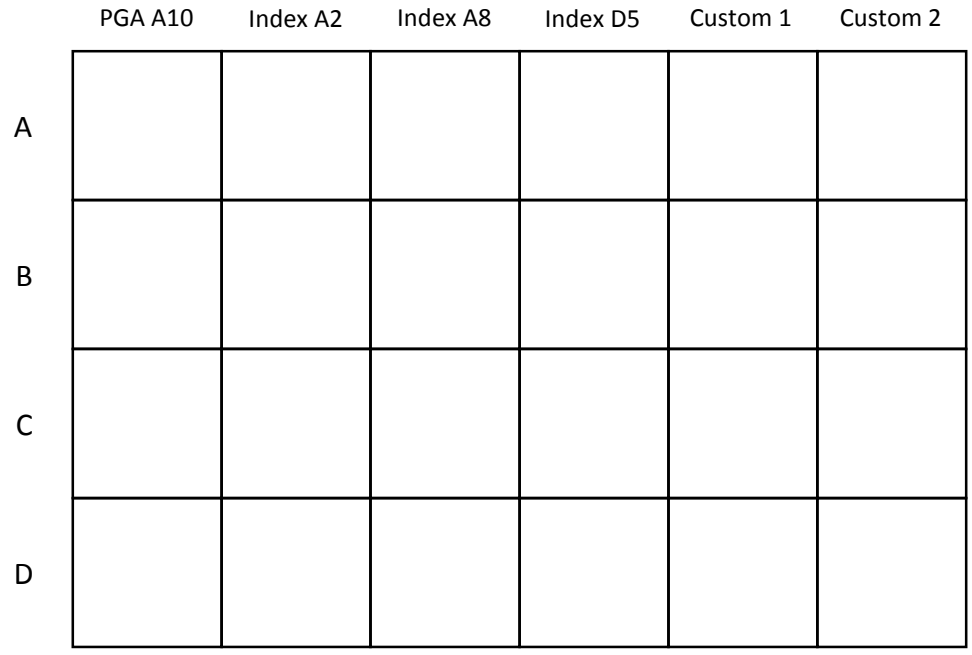

Figure 54: Crystal screen Custom α, using 30 mg/ml ΔCT694. A = 0.1% (w/v) octyl -D-glucopyranoside, B = 10 mM LDAO, C = 5 mM SB-12, D = 1:200 C_8E_5

02/06/15 - Custom β [Detergents] (30 mg/ml) 24-well:

	PGA A10	Index A2	Index A8	Index D5	Custom 1	Custom 2
E						
F						
G						
H						

Figure 55: Crystal screen Custom β, using 30 mg/ml ΔCT694. E = 0.2 M TMAO, F = 0.1 M NDSB 201, G = 1:333 Brij-30, H = 1:10 C12 POC

11/06/15 – Custom γ [Diluted detergents] (6 mg/ml) 24-well:

	PGA A10	Index A2	Index A8	Index D5	Custom 1	Custom 2
A						
B						
C						
D						

Figure 56: Crystal screen Custom γ, using 6 mg/ml ΔCT694. A = 0.017% octyl –D-glucopyranoside, B = 1.67 mM LDAO, C = 0.833 mM SB-12, H = 1:60 C12 POC

11/06/15 – Custom δ [Diluted detergents] (6 mg/ml) 24-well:

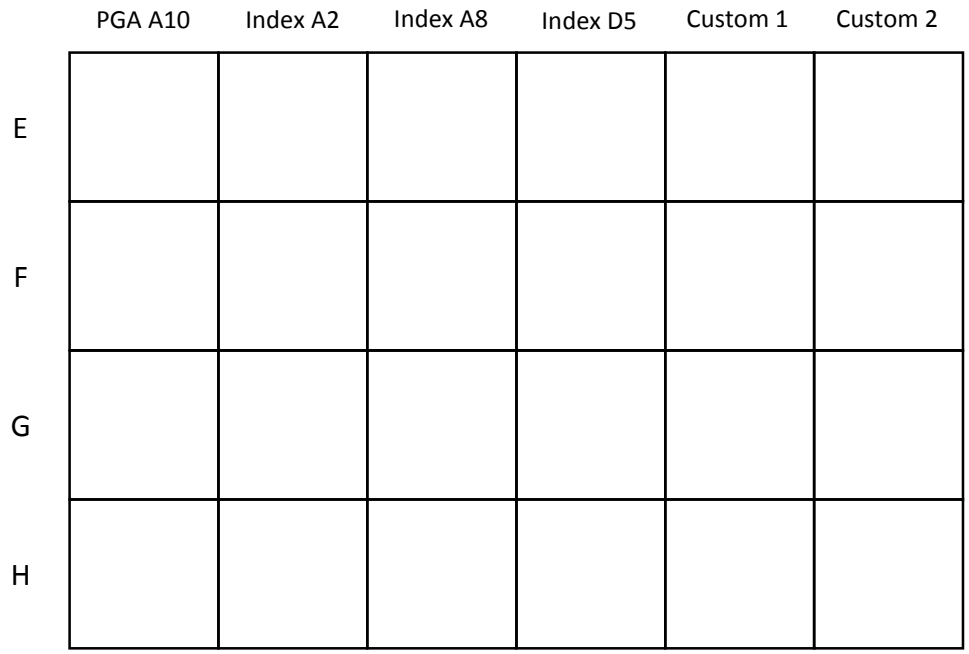

Figure 57: Crystal screen Custom δ, using 6 mg/ml ΔCT694. E = 20 mM TMAO, F = 10 mM NDSB 201, G = 2 mM TCEP, H = 5 mM DTT

26/06/15 – Custom CM (30 and 6 mg/ml) 6-well (12 drops):

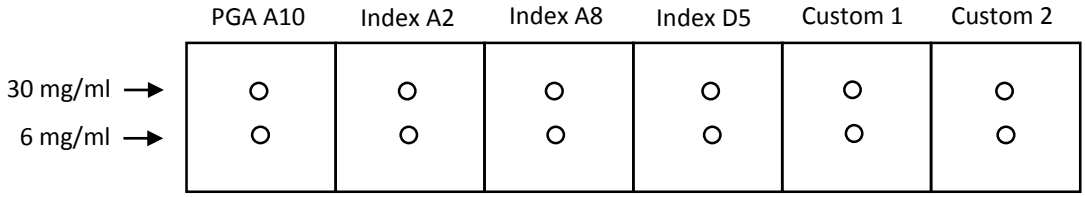

Figure 58: Crystal screen Custom CM, using 6 and 30 mg/ml carboxymethylated CT694 in separate drops in each well.

10/07/15 - Custom X [ML dilutions, ±glycerol, ±CM] (30 or 15 mg/ml) 24-well (48 drops)

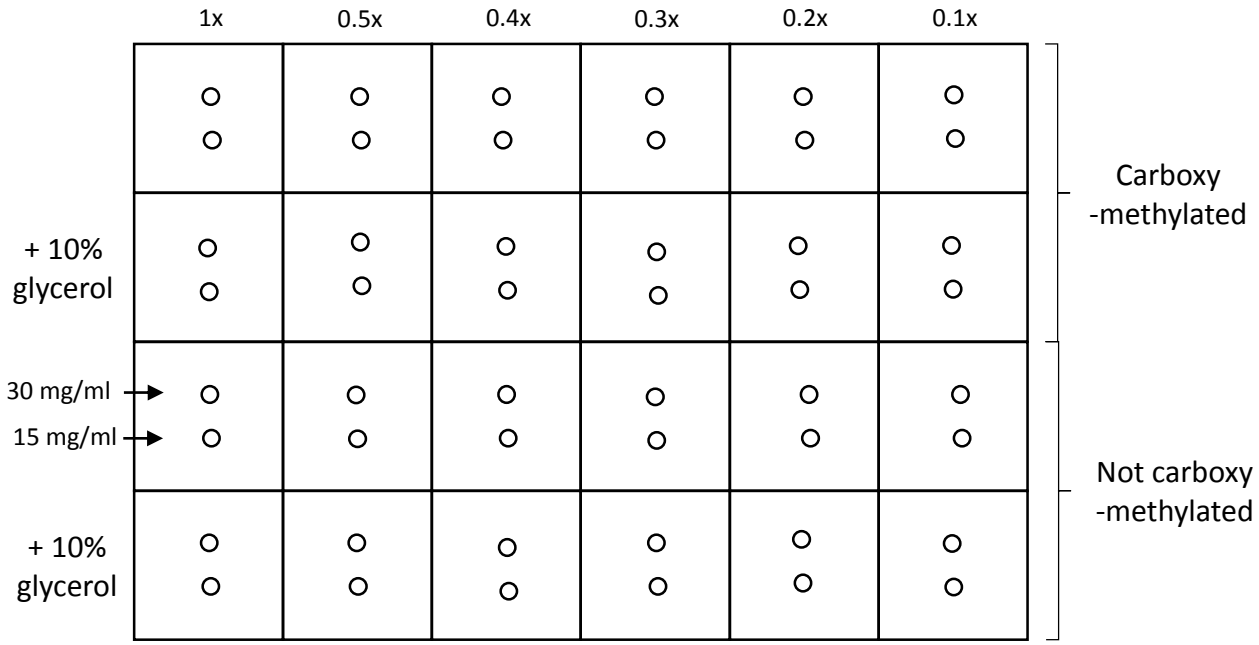

Figure 59: Crystal screen Custom X, diluting the mother liquor Index A8 in a gradient from left to right, using 15 and 30 mg/ml CT694 in separate drops in each well. Both carboxymethylated and non-carboxymethylated protein were used, as well as an addition of 10% glycerol.

3.0 - Results

3.1 - PCR and gene cloning

3.1.1 - ΔCT694

Figure 13 shows the first successful PCR agarose gel for ΔCT694 under UV light, to visualise the DNA in the gel after being run. PCR product was deposited directly into the wells at the top of the gel. The arrow shows the amplified band at its expected kilobase number (0.75 kb). This was then taken forward for double digest and ligation, after being cut out and gel purified.

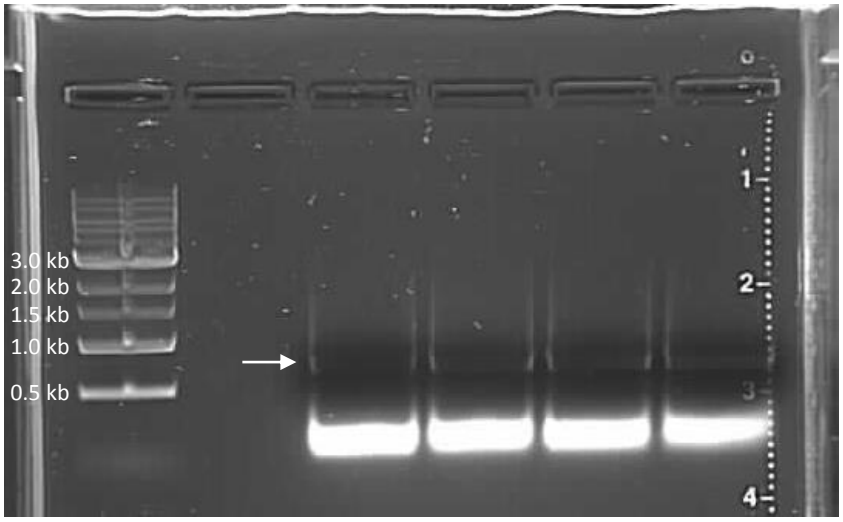

Figure 60: Successful PCR of ΔCT694. Far left well contained DNA ladder, and the four wells on the right contained PCR product. The arrow indicates the amplified DNA band, as expected at 0.75 kb.

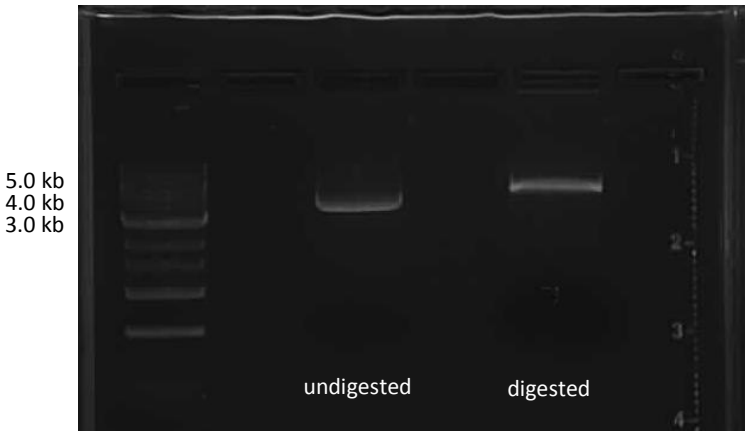

Figure 61: Test to determine whether digestion of pET28b vector was successful. The well on the far left contains DNA ladder. The digested plasmid appears to be at a higher molecular weight than the undigested plasmid.

Figure 14 shows a test to determine whether a digestion of plasmid vector is successful or not. The vector should run through the gel at a slightly higher apparent molecular weight when cut, which it did in this case. The cut vector was then gel purified for use in ligation with the ΔCT694 insert.

After ligation, the complete plasmids were used to transform NovaBlue GigaSingles competent cells and grown overnight on agar plates. Colony PCR was then performed using the colonies which formed. Figure 15 shows the agarose gel analysing the CPCR results. The bands are fairly faint but they are at the correct kilobase number and are pure, so this was considered a success. These colonies were used for Miniprep to obtain the DNA, which was then used to transform an expression strain (BL21 Gold).

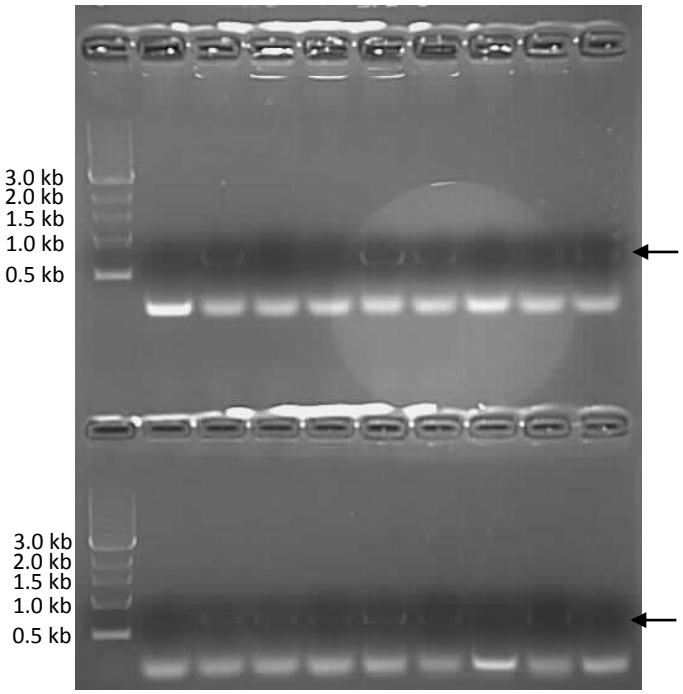

Figure 62: Successful CPCR of ΔCT694. The left hand wells contained DNA ladder, and the rest all contained PCR product from different colonies. The arrows indicate where the 0.75 kb amplified band was expected to appear, as it did in samples from most colonies.

3.1.2 - CT166

The DNA which CT166 was cloned from was a fragment of the full length gene, which does not include a putative signal sequence. Fewer problems were encountered when cloning CT166 than with ΔCT694; BL21 expression strain *E. coli* transformed with complete CT166 plasmid were obtained just over a week into the project. Figure 16 shows the agarose gel produced after a successful colony PCR performed with GigaSingles cells after the initial transformation. Colonies 1 to 3, 6 to 8, 11, 13 and 14 all contain a strong band at the correct kilobase number for CT166 (1.7 kb), and were used for Miniprep followed by transformation of BL21 expression strain bacteria.

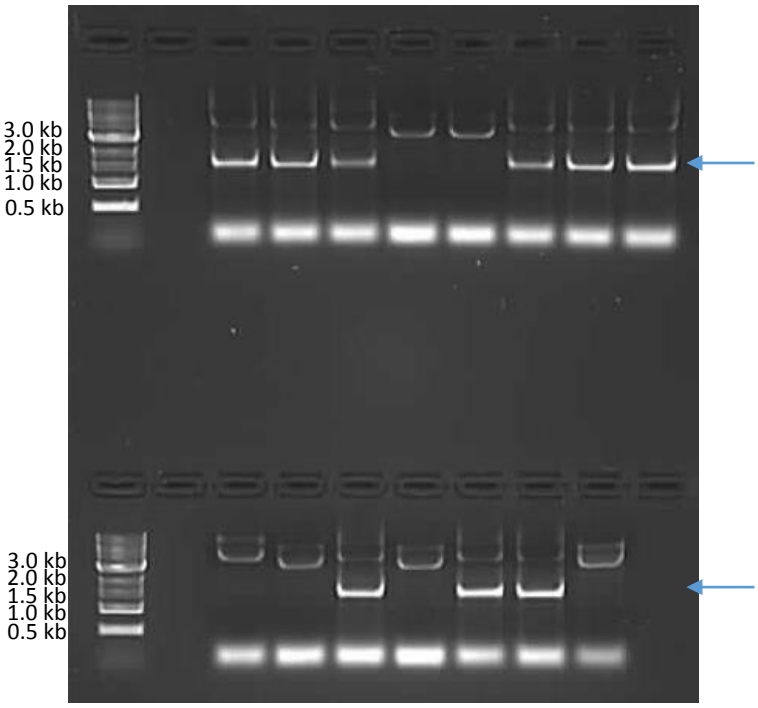

Figure 63: Successful CPCR of CT166. The left hand wells contained DNA ladder, and the wells on the right all contained PCR product from different colonies. The arrows indicate where the 1.5 kb amplified band was expected to appear, as it did in samples from most colonies.

3.2 - Expression and purification

3.2.1 - ΔCT694

After transformation of expression strains, a small-scale expression test was performed, in which the protein expression was compared of cells either induced with IPTG, or not. The SDS-PAGE gel for analysis is shown in Figure 17, after being stained and destained to show the protein bands in the gel. There was a clear increase in protein level at about 30 kDa between uninduced and induced cells, which showed the expression system worked correctly.

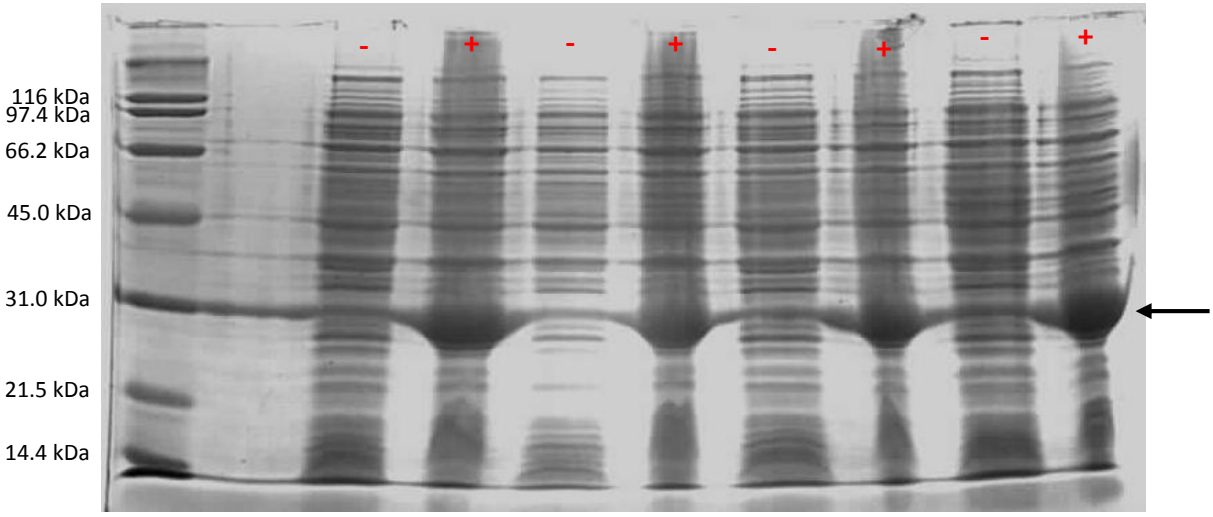

Figure 64: Small-scale expression test of ΔCT694. A minus sign indicates uninduced cells, a plus sign indicates induced cells. ΔCT694's molecular weight is labelled with an arrow (30 kDa).

The next step was large-scale expression. 6 L of cells were grown up per batch for harvest and purification, compared to about 100 ml total for the small-scale expression test.

Figures 18 and 21 are examples of UV traces formed when eluting ΔCT694 from nickel affinity columns using an AKTA purification system. The peak of ΔCT694 signal usually centred at around 20% buffer B, or 0.2 M imidazole using 1M imidazole in Ni buffer B, and usually approached 2 AU in strength which was close to the limit of upper range of the UV detector. The two fractions containing the ΔCT694 peak were taken forward for size exclusion chromatography in all cases, with other eluted peaks or signals being collected for SDS-PAGE analysis.

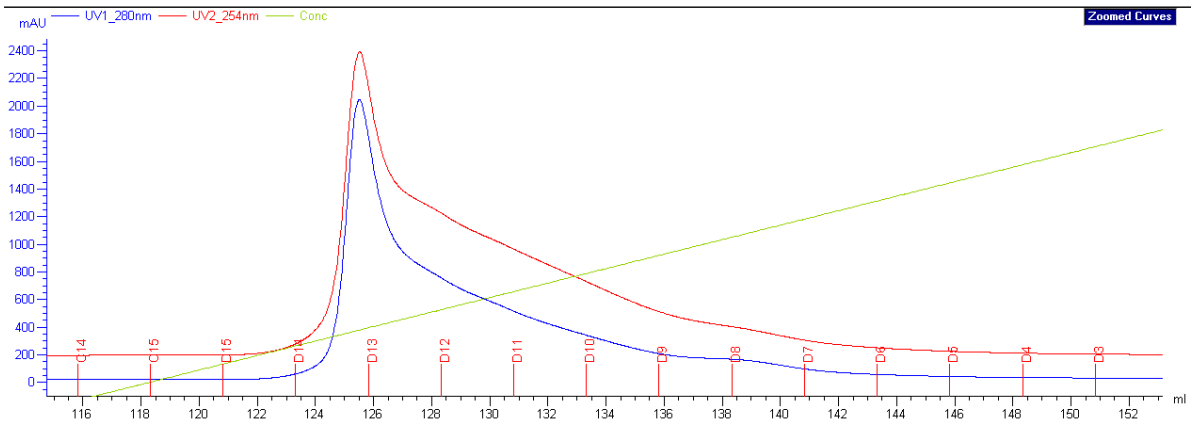

Figure 65: Example 1 of 2 of a Ni column UV trace for ΔCT694 (6th Nov 2014). The green gradient line indicates the increasing imidazole concentration. The red and blue UV traces show a peak of protein eluting from the column as this happens (mostly eluting into fractions D14 and D13).

Figures 19 and 22 are examples of UV traces formed when running ΔCT694 through a size exclusion column. As expected, larger or more oligomeric/aggregated material eluted first at around 40 ml, followed by ΔCT694 which usually eluted at around 60 to 70 ml. SDS-PAGE samples were taken of both peaks, mainly to ensure that the ΔCT694 was pure enough and did not need another purification step such as ion exchange chromatography.

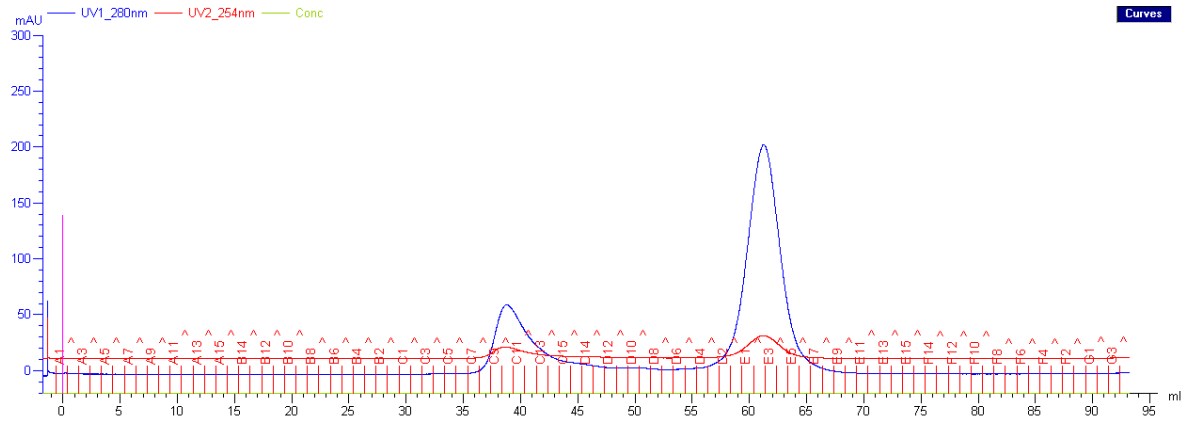

Figure 66: Example 1 of 2 of a size exclusion UV trace for ΔCT694 (6th Nov '14), using a S75 16/60 Superdex column. The blue peaks indicate protein eluting off the column.

Figure 20 is a picture of the SDS-PAGE gel run of all the samples taken for analysis during the purification of the ΔCT694 batch made in early November 2014, in order of when each sample was taken. As expected there is a trend going from left to right where the ΔCT694 protein lost more and more impurities with each purification stage. Well 10 shows the pooled protein from the size exclusion column (fractions D2 to E6) which was very pure, compared to the nickel affinity column elution shown in wells 5 and 6, containing only a few very dilute impurities.

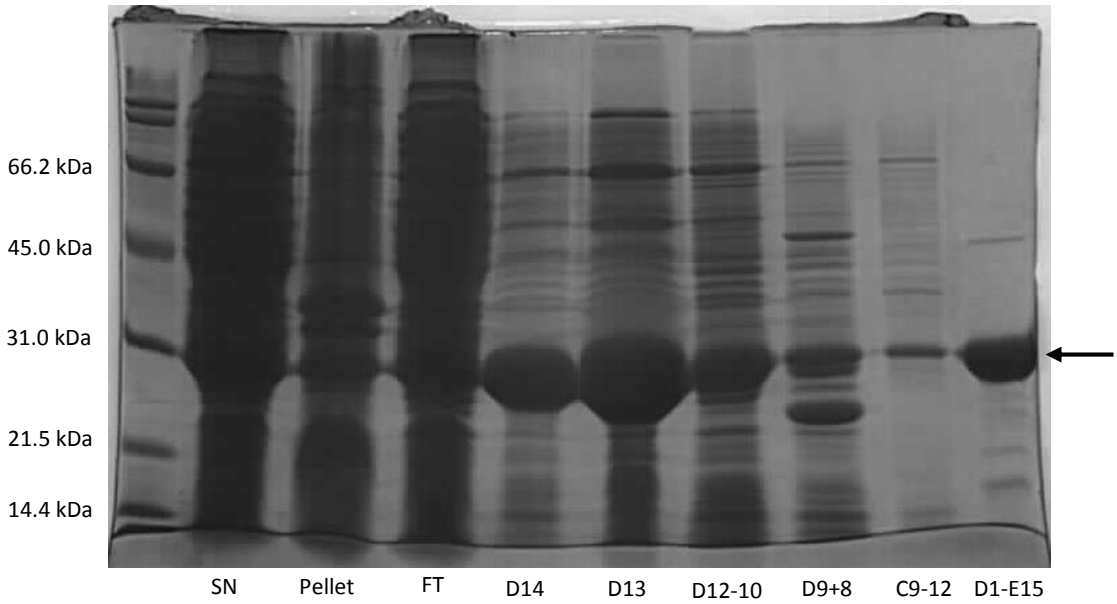

Figure 67: Corresponding SDS-PAGE gel of the 6th Nov '14 purification, showing pure ΔCT694 as the final product (D1-E15). SN = supernatant, Pellet = lysate pellet, FT = Ni flowthrough. D14, D13, and D12-8 are all nickel column fractions, C9-12 and D1-E15 are size exclusion fractions.

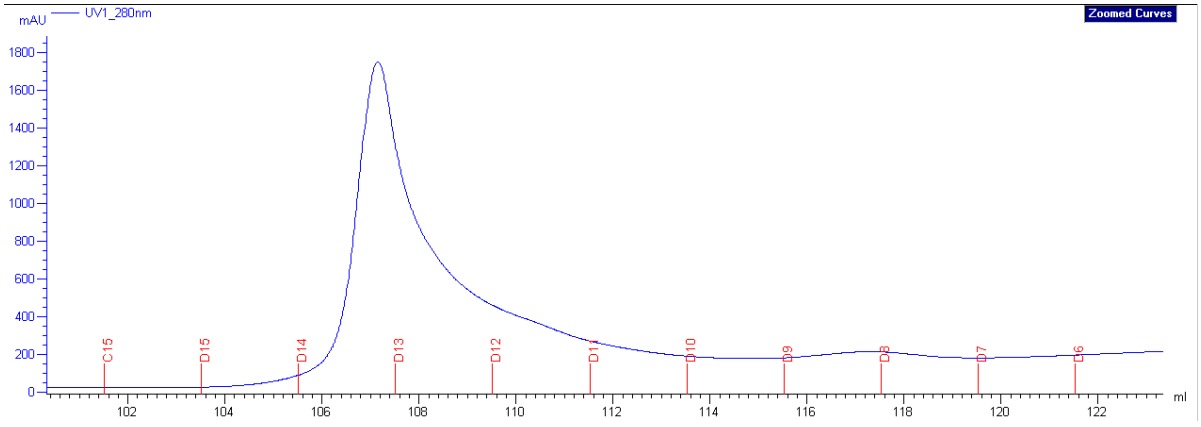

Figure 68: Example 2 of 2 of a Ni column UV trace for ΔCT694 (15th Jan 2015). The trace shows protein eluting in a relatively sharp peak into fractions D14 and D13.

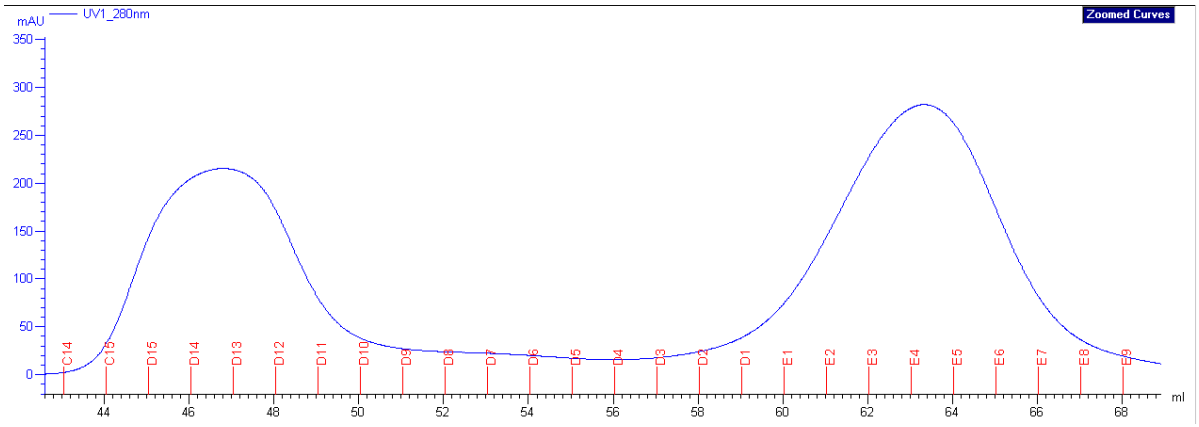

Figure 69: Example 2 of 2 of a size exclusion UV trace for ΔCT694 (15th Jan '15), using a S75 16/60 Superdex column. The blue peaks indicate protein eluting off the column. The peaks appear broad due to this trace being zoomed in to focus on the peaks and show fractions clearly.

Figures 23 and 24 show the gel electrophoresis analysis of the ΔCT694 batch produced mid-January 2015. Figure 23 is a picture of a SDS-PAGE gel similar to Figure 20 in that it is in chronological order of samples. The protein band profile above 30 kDa in well 9, which is the fraction pool of the early peak from the size exclusion column, is very similar to that of the nickel affinity column elution (well 5), but is completely absent from well 10, which corresponds to the later size exclusion peak containing the majority of the ΔCT694. This demonstrates the functionality of size exclusion columns in this field very well: separating larger protein molecules from smaller ones effectively. The yield in this purification was not quite as pure as the November batch (Figure 20), containing a thicker band of impurity at about 25 kDa.

Figure 24 is a picture of a native gel, in which the oligomeric state of the peaks collected from the size exclusion column was analysed. The right hand well shows the early peak, which is clearly quite aggregated as expected, whereas the later ΔCT694 peak is mostly monodisperse.

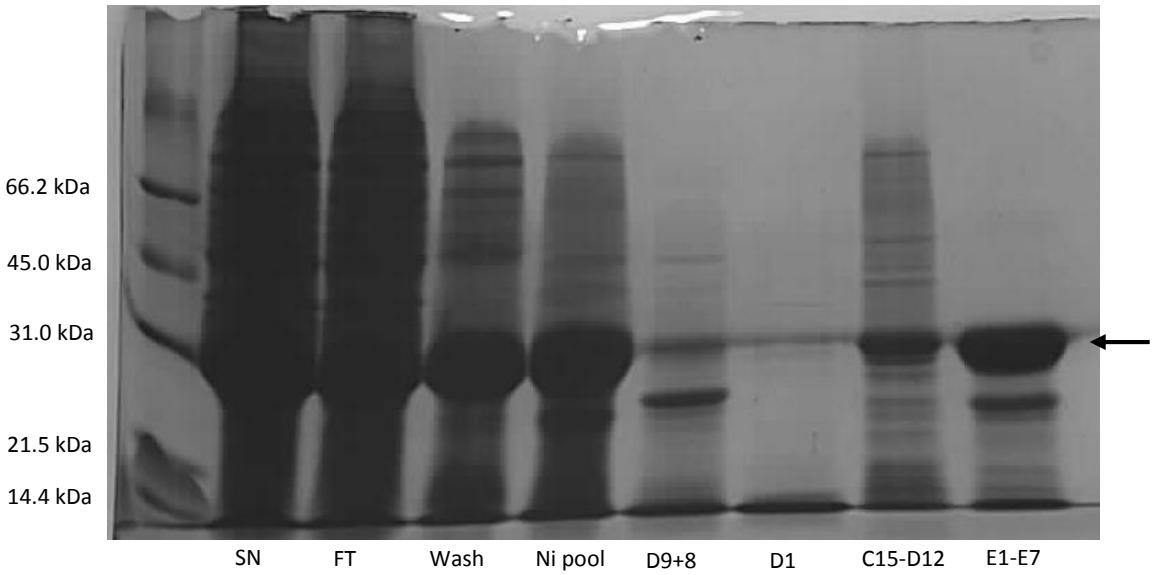

Figure 70: Corresponding SDS-PAGE gel of the 15th Jan '15 purification, showing pure ΔCT694 as the final product. Wash = a sample taken after washing the column post-protein loading, Ni pool = fractions to be loaded onto size exclusion pooled together. D9+8 and D1 are nickel column fractions, C15-D12 and E1-E7 are SEC fractions.

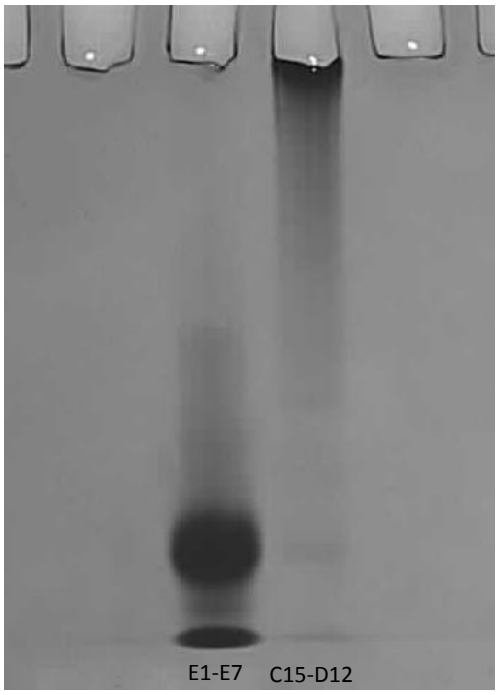

Figure 71: Native gel comparison between size exclusion fractions from the 15th Jan '15 purification. Fractions E1-7 appear to contain mostly monomeric protein, whereas C15-D12 appear to contain mostly oligomer.

Figure 25 shows a nickel column elution after a carboxymethylation process had been performed. The high UV signal at the beginning is caused by iodoacetic acid still being present on the column; one can see the signal disappear rapidly after about 5ml of washing has occurred, and fractions A1+2 were tested on a SDS-PAGE gel (Figure 26) and were found to have no protein in them. Figure 26 is a picture of an SDS-PAGE gel comparing ΔCT694 before and after carboxymethylation; there appears to be very little change in concentration and purity.

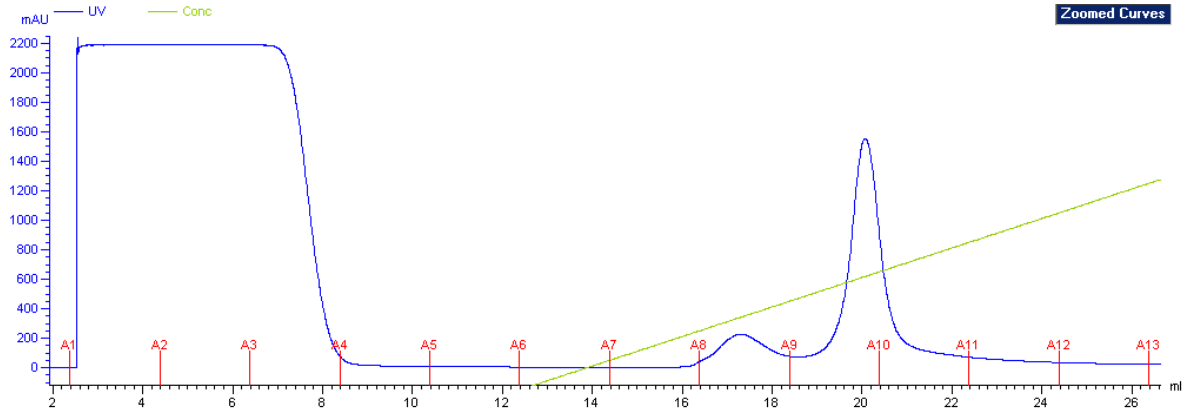

Figure 72: Ni column UV trace of carboxymethylated ΔCT694 being eluted after the process (25th Jun '15). The large signal from 2 to 8 ml is caused by iodoacetic acid being washed from the column before the imidazole gradient (the green line) was started.

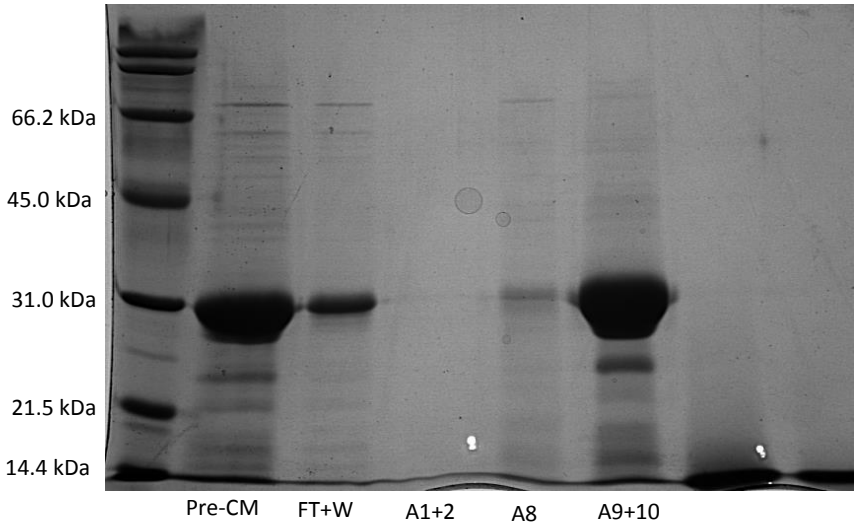

Figure 73: SDS-PAGE gel to determine how much ΔCT694 was lost during the process (result: little). Pre-CM = protein before the carboxymethylation process, FT+W = flowthrough and initial column wash pooled together.

3.2.2 - CT166

After transformation of BL21 expression strain with the CT166 gene, a small-scale expression test was performed. The SDS-PAGE gel for analysis is shown in Figure 27. There was a clear increase in protein level at about 66 kDa between uninduced and induced cells, which showed the expression system worked correctly (the lower molecular weight is due to the shortened gene cloned, not including a signal sequence from the full length gene).

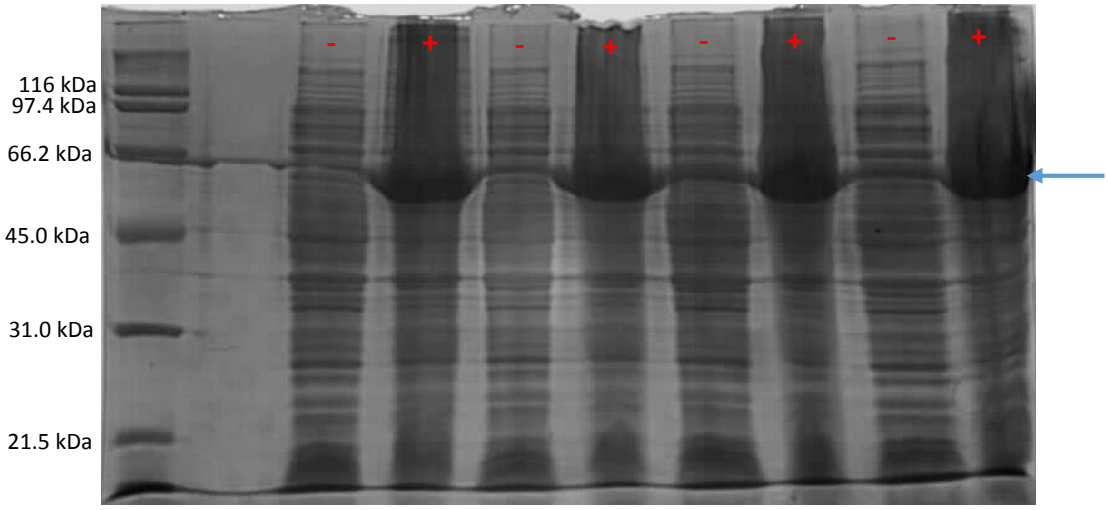

Figure 74: Small-scale expression test of CT166. A minus sign denotes uninduced cells, a plus sign denotes induced cells.

The expression process was scaled up to produce a batch of CT166 protein, using a similar harvest and purification protocol to ΔCT694. Figure 28 shows the UV trace from the nickel column elution of the first batch of CT166 attempted. Fraction A11 (5 ml) was taken forward for size exclusion purification, followed by flash freezing and storage. The peak is quite wide compared to the average ΔCT694 peak.

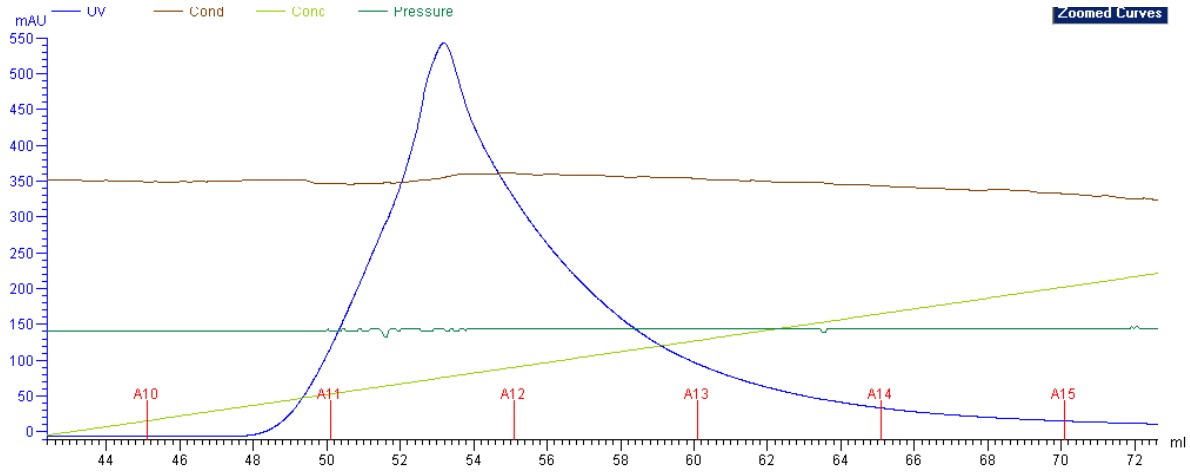

Figure 75: Ni column UV trace for CT166 (11th Sep '14). The blue line shows a peak in signal as protein elutes from the column.

Samples taken during the purification were analysed on a SDS-PAGE gel, shown in Figure 29. The concentration of protein is lower than ΔCT694, and the relative concentration of impurities with respect to the concentration of the target protein is higher. The amount of protein produced by the cells is very large, but little seems to have entered the supernatant, and the majority appears to be in the cell pellet (well 3).

Figure 30 shows the native gel analysis of the fractions from the size exclusion column. It appears to suggest that all of the CT166 which eluted from the column is oligomeric or aggregated. This may not be the case as it was noted that the isoelectric point of CT166 is 6.83, which is very similar to the pH in the native gel (6.8). Since the protein is not charged, it may simply not move with the current when running the gel. Further experiments are needed to confirm this theory.

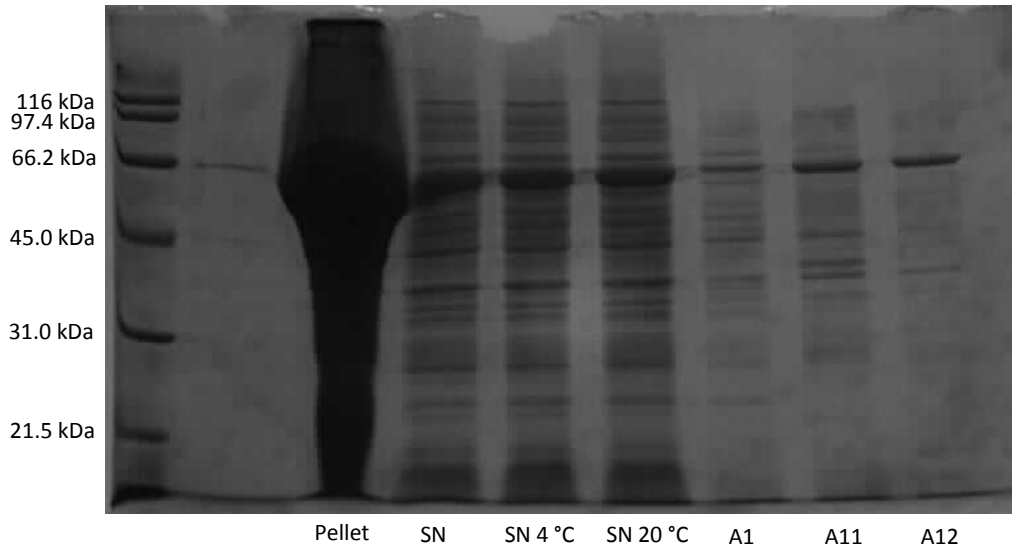

Figure 76: Corresponding SDS-PAGE gel of the 11th Sep '14 purification, showing pure, but dilute CT166 as the final product. SN 4 °C = supernatant stored in the fridge over four nights and then tested. SN 20 °C = the same but at room temperature.

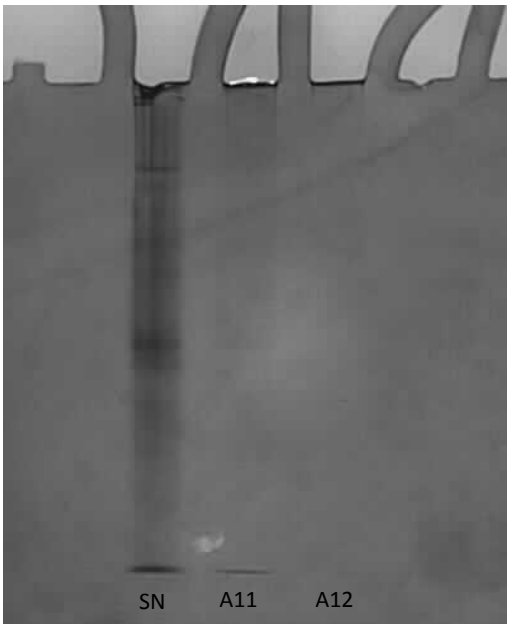

Figure 77: Native gel appearing to show that CT166 eluted from the Ni column is almost entirely oligomeric or aggregated.

3.2.3 - PmpD F2

PmpD F2 was already cloned and a protocol for expression and purification was already in place from a previous project, involving inclusion body prep and on-column refolding. Figure 31 shows a nickel column elution UV trace after on-column refolding. The peak is again quite wide compared to the nickel UV peaks seen from ΔCT694, and has a much lower peak UV reading even though the final concentration of protein was usually similar to ΔCT694 (0.5-2.0 mg/ml).

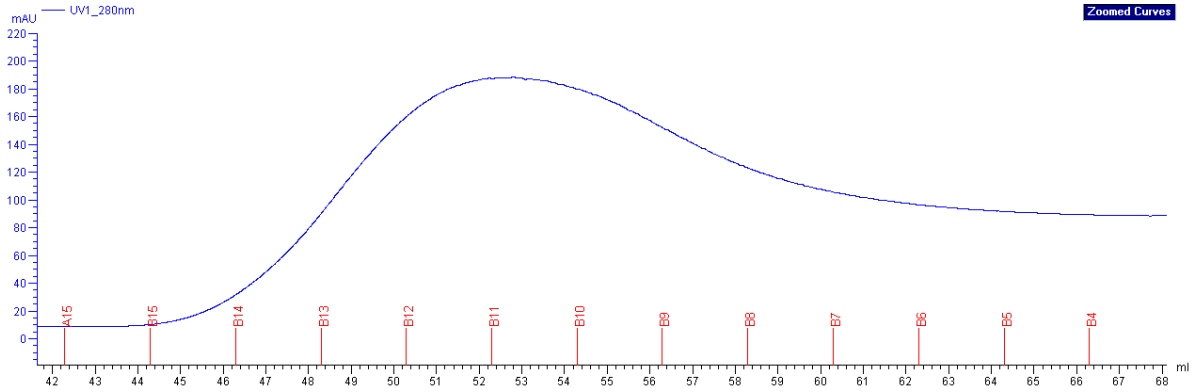

Figure 78: Example of a Ni column UV trace for PmpD F2 (23rd Jan '15). The peak is noticably broader compared to typical ΔCT694 UV traces.

As with ΔCT694 and CT166, the PmpD F2 fractions (B12 and B11 in this case) were pooled for size exclusion chromatography. Figures 32 and 35 show UV traces, Figure 32 being the size exclusion trace corresponding to the nickel column run in Figure 31. Usually, two peaks formed with some merging in the middle. The earlier peak, usually starting to form from 40-50 ml, was the oligomer (OLIG) of PmpD F2 and the later peak, usually peaking between 70 and 80 ml, the monomer (MON), with the peak merge containing an intermediate mixture of the two (INT). Fractions were taken accordingly and the peaks kept separate.

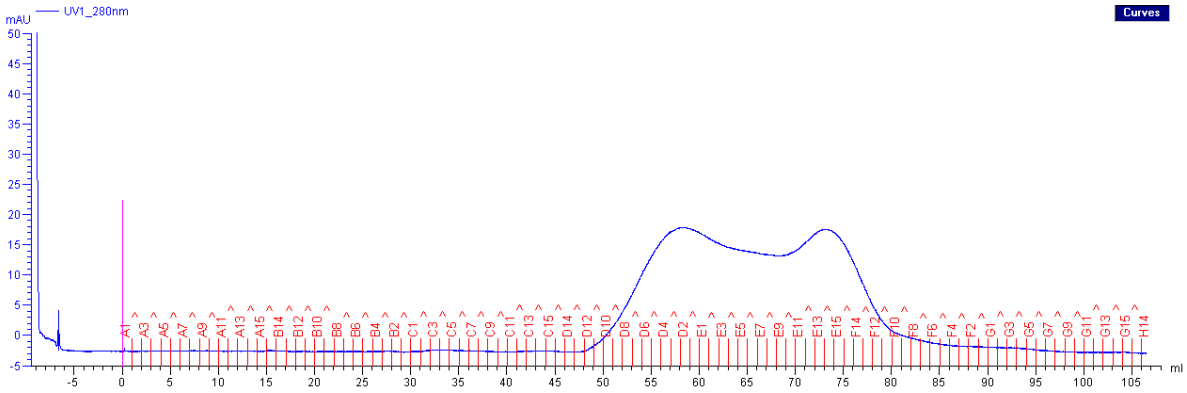

Figure 79: Example 1 of 2 of a size exclusion UV trace for PmpD F2 (23 Jan '15), using a S200 16/60 Superdex column. The blue peaks indicate protein eluting off the column. The peaks merge noticeably with some intermediate material eluting from the column.

Samples taken during purification were used in SDS-PAGE analysis, a gel picture of which is shown in Figure 33. The final PmpD F2 protein (65 kDa) was pure and a useful amount was yielded. Figures 34 and 36 show native gel analysis of the size exclusion fractions. The difference in the size exclusion peaks can be seen very well in both gels; the OLIG fraction (D9-D1) hardly enters the gel, the MON fraction (E13-F12) flows through the gel well and the INT fraction (E2-11) appears to be a mixture of different states of oligomerisation, forming a long streak.

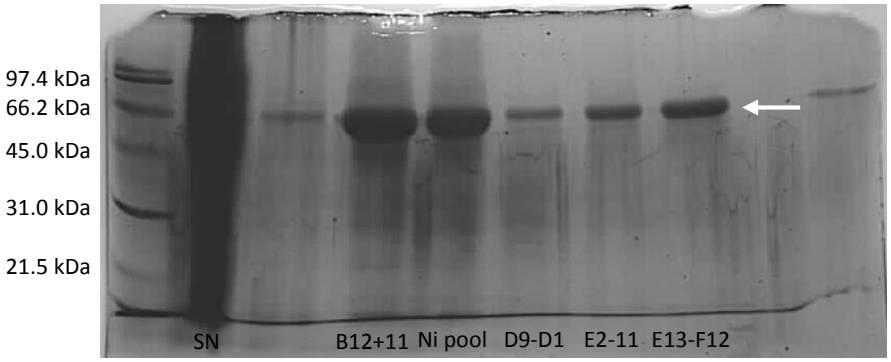

Figure 80: Corresponding SDS-PAGE gel of the 23rd Jan '15 purification, showing pure PmpD F2 as the final product. B12+11 and Ni pool are nickel fractions, the other three (wells 6-8) are SEC fractions.

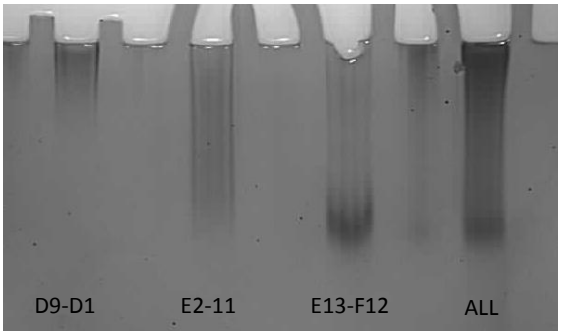

Figure 81: Native gel showing the different oligomeric states of PmpD F2 eluting from the size exclusion column: OLIG (D9-D1), INT (E2-11) and MON (E13-F12). ALL is a mix of the three.

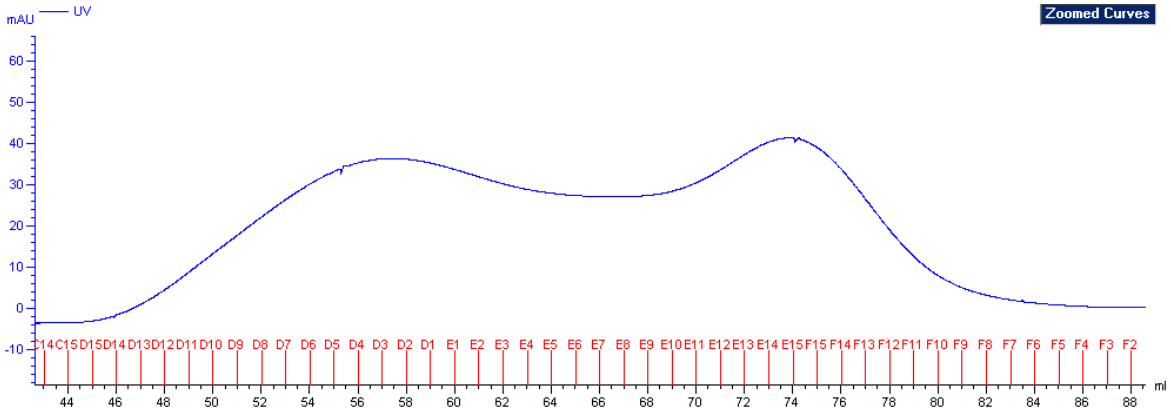

Figure 82: Example 2 of 2 of a size exclusion UV trace for PmpD F2 (17th Apr '15), using a S200 16/60 Superdex column.

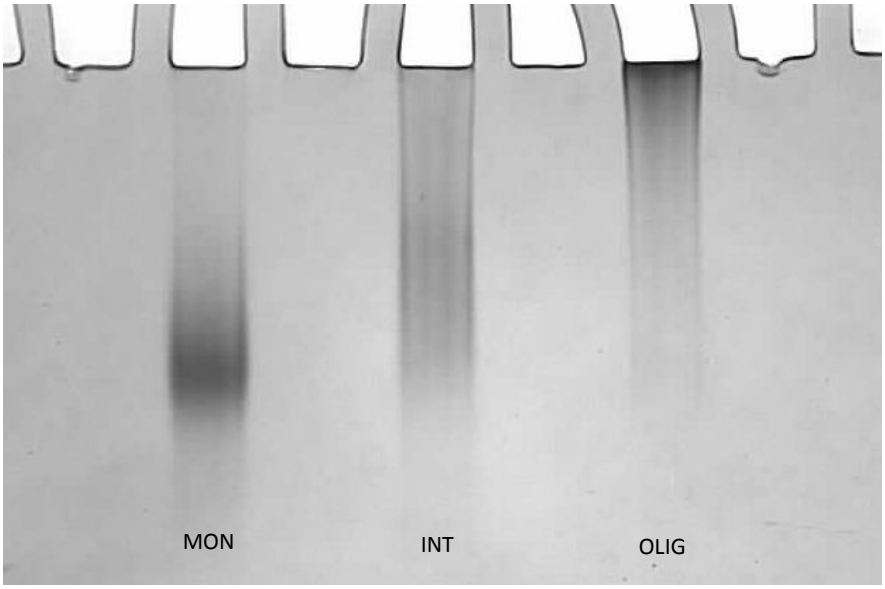

Figure 83: Native gel of the 17th Apr '15 purification showing the different oligomeric states of PmpD F2 eluting from the size exclusion column.

3.3 - Experiment results

3.3.1 - ΔCT694

After primary and secondary screening of ΔCT694 with crystallisation conditions and multiple custom screens performed, Figures 37 and 38 show the best condition identified, containing 30 mg/ml ΔCT694, 30 mM NaOAc (pH 4.5) and 0.9 M NaCl. The drop contains a fine microcrystalline residue, which is promising but could be seen in many conditions which were tested. These conditions were altered in an effort to trigger full crystal growth, but this did not occur.

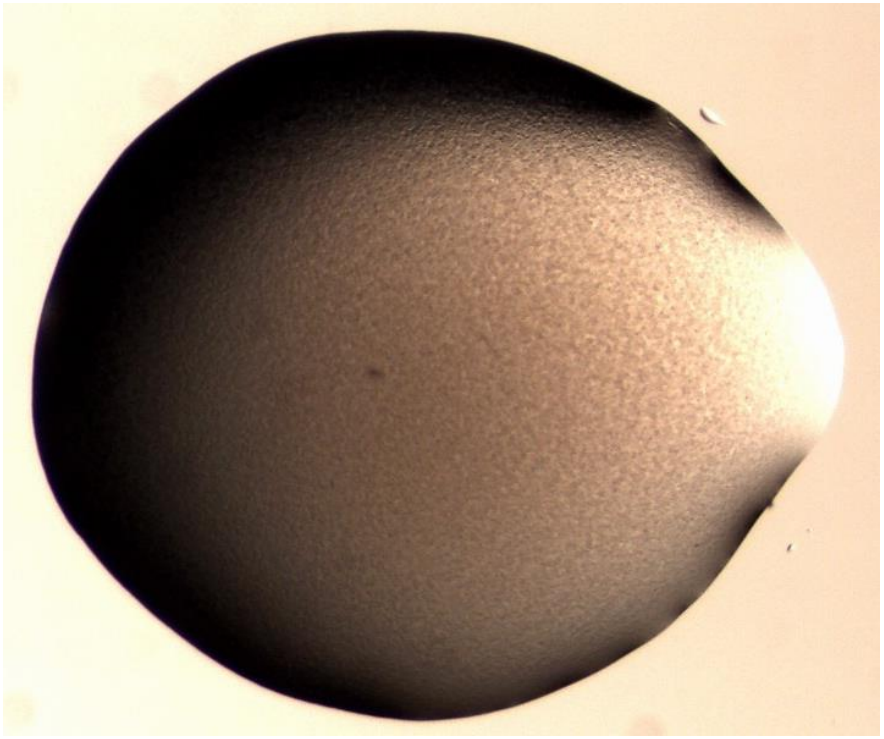

Figure 84: The best condition achieved from crystallisation trials over the course of this project.

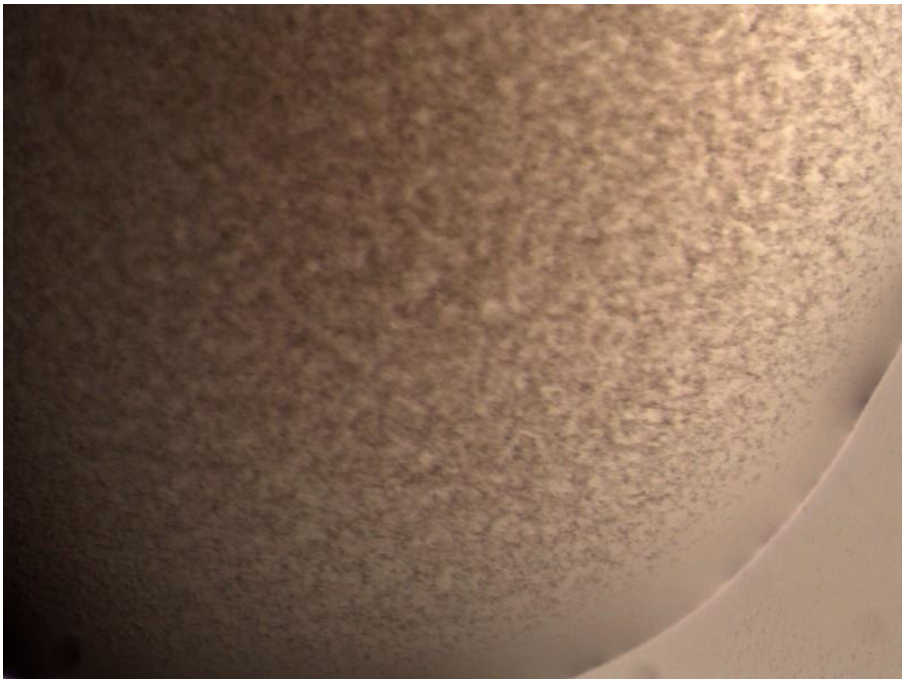

Figure 85: A zoomed view of the microcrystalline structure in the crystal drop.

3.3.2 - PmpD F2

The effect of reducing agents on PmpD F2 was investigated. Figures 39 and 40 show native gels run after incubating PmpD F2 with high and low concentrations of reducing agents:

- DTT: High = 50 mM, low = 10 mM
- TCEP: High = 25 mM, low = 2.5 mM
- βME: High = 0.5 M, low = 50 mM

The expected result was that conditions with reducing agent, especially at high concentration, would flow through the gel more readily. Instead, the opposite appeared to happen, in that the presence of reducing agent caused PmpD F2 to not flow through the gel; this is easily seen in Figure 39 when comparing the control lane to the others.

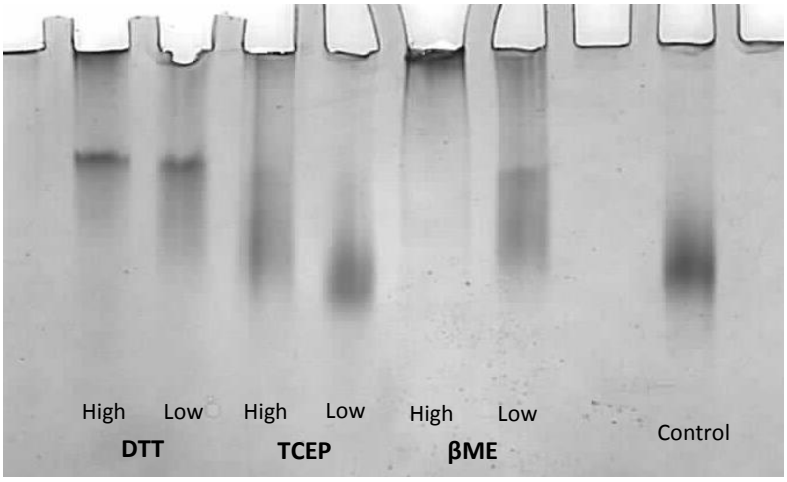

Figure 86: Native gel showing the effect of high and low concentrations of reducing agents on monomeric PmpD F2.

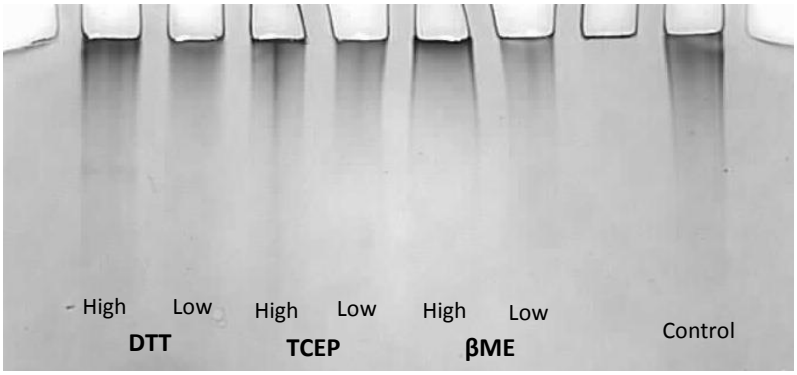

Figure 87: Native gel showing the effect of high and low concentrations of reducing agents on oligomeric PmpD F2.

The effect of different pH levels on PmpD F2 was also investigated. PmpD F2 monomer and oligomer were incubated in buffers of different pHs ranging from 3 to 10 for 1 h, then run on a SDS-PAGE gel for analysis (Figures 41 and 42). There seemed to be no change in the state of monomeric or oligomeric PmpD F2 at any pH.

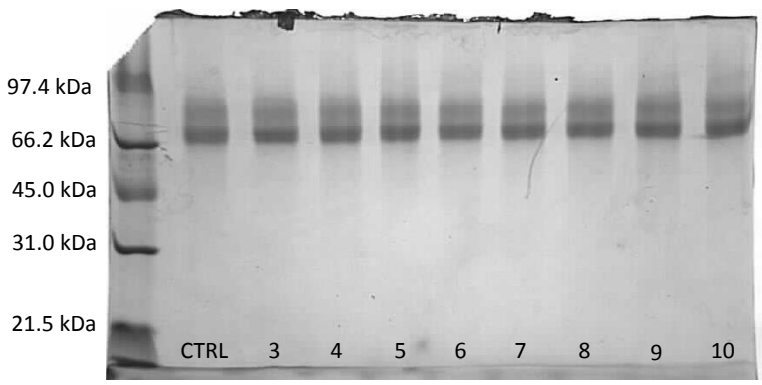

Figure 88: SDS-PAGE gel showing the effect of different pH levels on monomeric PmpD F2.

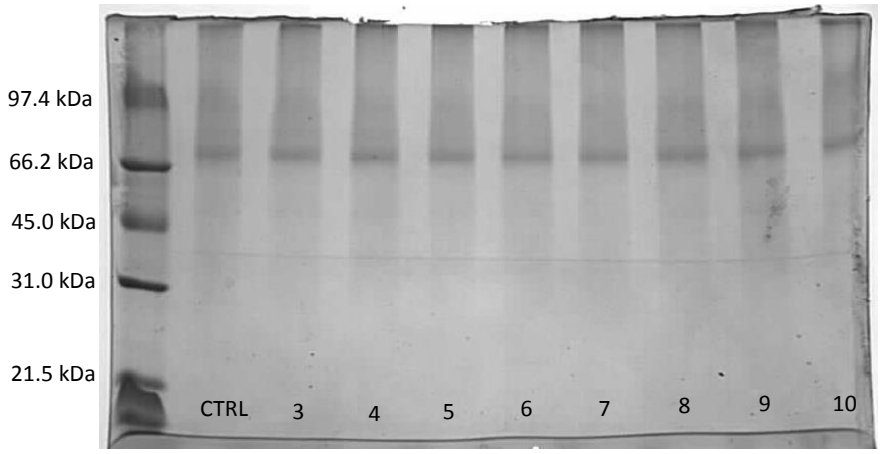

Figure 89: SDS-PAGE gel showing the effect of different pH levels on oligomeric PmpD F2.

Proteolysis of PmpD F2 was performed to determine if any stable fragments could be identified. In the first attempt, PmpD F2 monomer and oligomer at 20 mg/ml were incubated with trypsin and subtilisin for 5 min, 15 min, 30 min or 1 h, then the reactions were quenched with SDS-PAGE sample buffer and the samples were run on gels (Figure 43). This attempt was unsuccessful in that the incubation time was too long and/or the protease concentration was too high, leading to almost complete digestion in most conditions. The only discernible protein bands were seen in the 5 min timepoint with trypsin. Subtilisin is non-specific and so completely digested the protein in under 5 min.

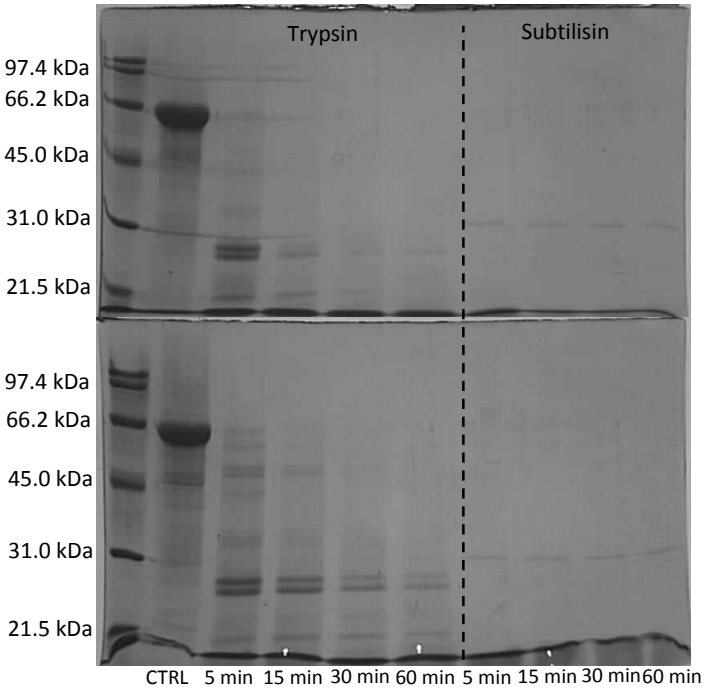

Figure 90: First attempt at proteolysis of PmpD F2 monomer (gel 1) and oligomer (gel 2) with trypsin and subtilisin.

In the second attempt, the incubation timepoints were reduced to 30 s, 2 min, 5 min and 30 min, and the proteases were diluted 1:5 from the previous attempt. Subtilisin was not used, but chymotrypsin, clostripain and elastase (Hampton Research) were used alongside trypsin. These proteases were chosen after analysing how many sites of cleavage were predicted on PmpD F2 using the ExPASy web resource (SIB Bioinformatics).

Figures 44 and 45 show the SDS-PAGE analysis gels of monomeric and oligomeric PmpD F2 respectively. As expected, the PmpD F2 broke down much less than in the first attempt using the new timepoints and protease concentrations. Looking at the 30 min timepoint for trypsin, it was clear that oligomeric PmpD F2 was less prone to digestion than monomeric PmpD F2, which makes sense considering that oligomeric PmpD F2 has less surface area per monomer exposed to solution. Clostripain and chymotrypsin seemed almost inactive, so they may need their concentrations increasing or longer incubation times.

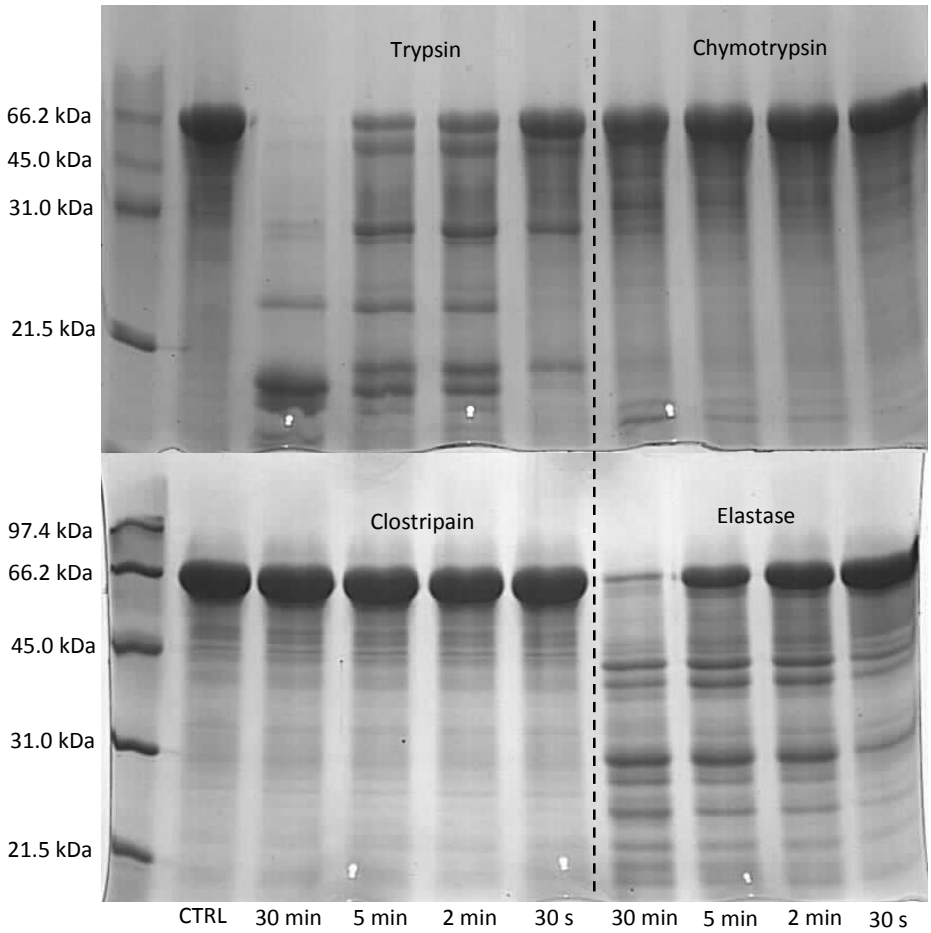

Figure 91: Second attempt at a proteolysis experiment for monomeric PmpD F2.

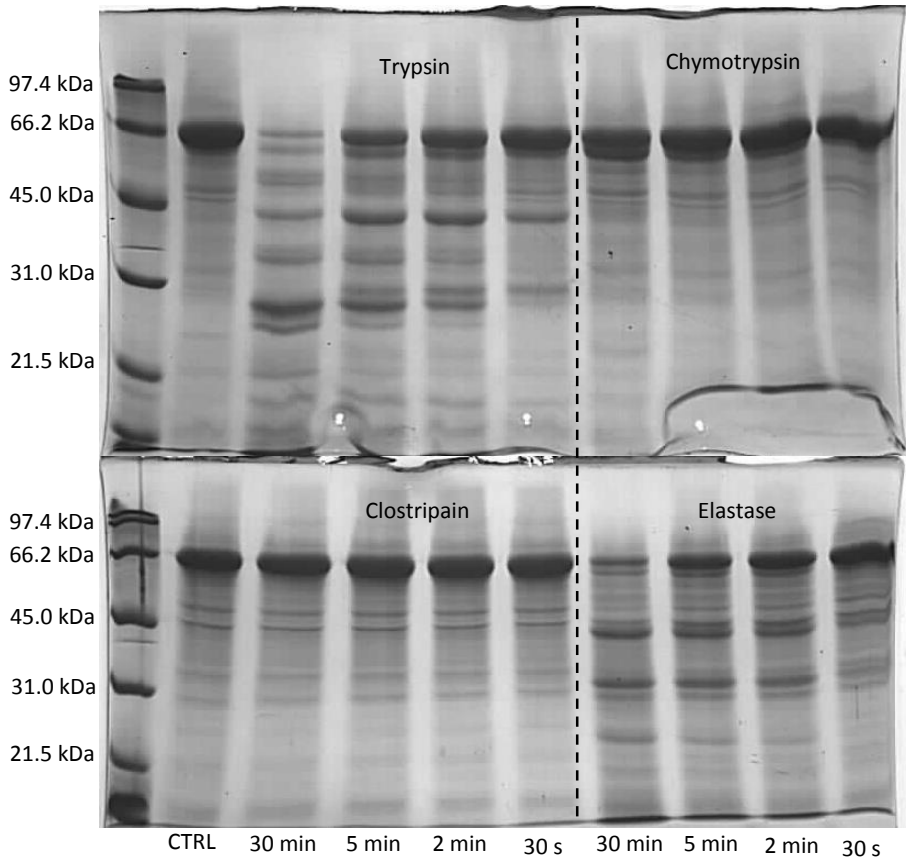

Figure 92: Second attempt at a proteolysis experiment with oligomeric PmpD F2.

4.0 - Discussion

4.1 - Purification and experimentation (COOMe etc.)

Once ΔCT694 had been successfully cloned and used to transform expression strains, with a small-scale expression test to confirm, the purification protocol which was put in place was similar to the one used to produce full-length CT694. This is because it worked well for the previous project and since ΔCT694 is a fragment of CT694, the protocol would also work well for this purification. Little optimisation was needed to produce a high yield of pure protein with each purification. The few differences between protocols included:

- Not concentrating the Ni column elution. This was to ensure that as much ΔCT694 as possible stayed monomeric, so as little as possible entered the higher molecular weight portion of the size exclusion elution which contains most of the impurities, and the lower molecular weight portion contained a high yield of pure ΔCT694. Also, some protein is lost in the concentration process.
- Removing the Mono-Q column ion exchange step. The protein collected from size exclusion was pure enough to not need another purification step. Ion exchange results in the protein eluting in a relatively high-salt buffer, which means buffer exchange to a lower salt concentration was necessary before the protein could be used in crystallisation screens. A step such as this being skipped also reduces decrease of protein yield, both during the column run itself and the buffer exchange step.

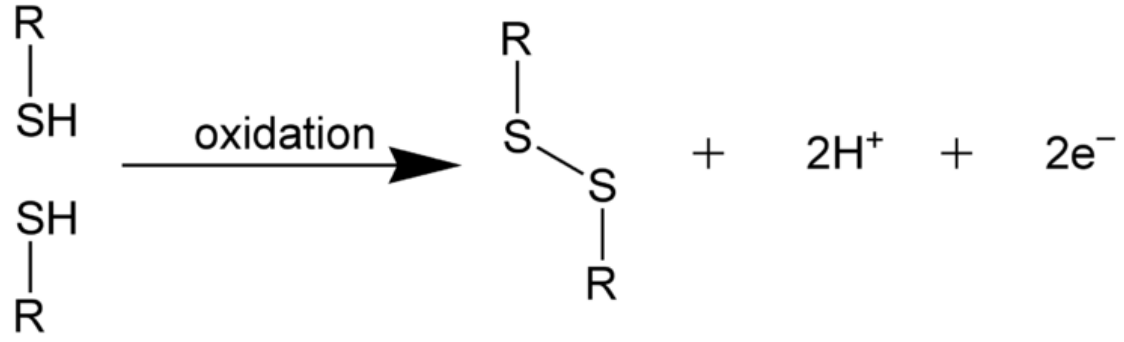

Figure 93: Mechanism for disulfide bonding. In the case of intra- or intermolecular protein bonds, the R groups are cysteine residues on the same or different proteins.

For the purpose of crystallisation conditions, the protocol was modified to include a carboxymethylation step. ΔCT694 contains two cysteine residues, and it is unclear whether these are involved in disulfide bonding (see Figure 46), either within the ΔCT694 molecule or with other protein molecules. Carboxymethylation is the process of chemically modifying the –SH group on each cysteine such that they are unable to form disulfide bonds with other cysteines. Iodoacetic acid (ICH_2COOH) is employed to react with the cysteines, it adds a carboxymethyl group to the sulfide atom, with hydrogen iodide as a biproduct (see Figure 47). Although this could have helped with crystal formation by producing a more monodisperse solution of ΔCT694, it is possible that the putative disulfide bonding is involved with forming secondary and tertiary structure in the protein, and so it could also have interfered with said structure and hinder the chances of crystal formation in screens.

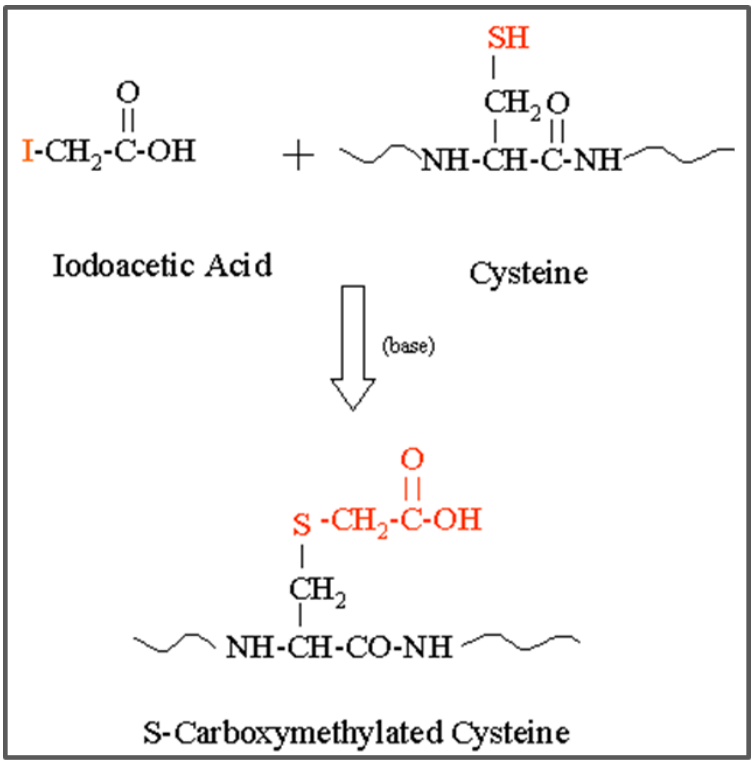

Figure 94: Mechanism of carboxymethylation of cysteine residues in proteins using iodoacetic acid[32].

PmpD is a membrane protein, which requires it to have a hydrophobic region with which to associate with the cell membrane. When overexpressed in bacterial cells, the protein is stored in insoluble inclusions in the bacterial cells. Therefore, purification of PmpD F2 requires a different protocol to CT694. Once the cell pellets had been acquired after lysis, the insoluble inclusions were dissolved in guanidium hydrochloride, which is a strong denaturant. A concentration of 6 M is enough to completely denature almost any protein. The concentration of GdmHCl was then

lowered gradually by dialysis of the protein into decreasing concentrations over a number of days, to allow the protein to slowly refold into a stable, somewhat soluble form. The protein, in theory, could then be purified normally using a similar method to ΔCT694.

It was expected that the majority of the purified PmpD F2 protein would be in an oligomeric form, not only because it is a membrane protein with a hydrophobic domain which could readily associate with other domains intermolecularly, but because it also contains a total of 23 cysteine residues which could form disulfide bonds with other protein molecules. However, there was an almost equal amount of monomeric and oligomeric protein, as seen in Figures 32 and 33. It is interesting to note that although PmpD has shown evidence of being readily proteolytically cleaved to produce different fragments, relative to full-length CT694 (which was thought to be quite stable), it does not degrade during purification. This is even after being exposed to very harsh denaturing conditions (6 M GdmHCl).

4.2 - Crystal screens

To begin the screening process, common 96-condition commercial screens were used from Hampton Research and Molecular Dimensions, including Index, PACT and Hampton 1and2, as well as others such as the PGA-LM screen developed by the York Structural Biology Laboratory. It was not expected that we would obtain usable crystals from this stage, but rather that these screens were a starting point to determine which conditions to take forward for customisation. These conditions ideally appeared to contain granular precipitate or even microcrystals, which would suggest that the condition is suitable for the protein to crystallise but certain variables in the condition need tweaking, for example salt concentration or pH. The conditions taken forward were:

- PGA-LM screen, well A10 (minus PGA)
    - 0.1 M sodium acetate (NaOAc), pH 5.0
    - 30% PEG 400 (v/v)
- Index screen, well A2
    - 0.1 M NaOAc, pH 4.5
    - 2 M ammonium sulfate ($(NH_4)_2SO_4$)
- Index screen, well A8
    - 0.1 M NaOAc pH 4.5
    - 3 M NaCl

- Index screen, well D5
    - 0.1 M NaOAc pH 4.5
    - 25% PEG 3350 (w/v)

These were chosen from a shortlist of conditions which contained granular precipitate. It was noted that the most common trait in all the conditions in the shortlist were that the buffer was 0.1 M NaOAc, with a pH between 4.5 and 5.0. These conditions were the basis of the subsequent customised screens which were performed, as well as two other custom conditions:

- Custom 1
    - 0.1 M sodium cacodylate (NaCac), pH 6.5
    - 2 M $(NH_4)_2SO_4$
- Custom 2
    - 0.1 M Tris, pH 8.5
    - 2 M $(NH_4)_2SO_4$

Using these conditions we performed various custom screens testing pH (Figures 5 and 6), screening detergent additives (Figures 7 to 10), using carboxymethylated protein (Figures 11 and 12), and diluting the mother liquor and testing the addition of glycerol (Figure 12). Initially we increased the protein concentration to 80 mg/ml, but it resulted in total precipitation, so we used lower concentrations for subsequent screens (usually 30 mg/ml). Using lower concentrations resulted in the same quality of precipitate forming, but with a lower amount of it. Varying pH and conventional additives did not seem to exert much of an effect on the protein. Most detergent additives seemed to have a negative effect on the quality of the precipitate, as did adding 10% glycerol. Carboxymethylating the protein made no discernible difference. However, diluting the buffer did improve the appearance of the precipitate slightly. The condition chosen as the best condition to use in the amino acid custom screen was:

- 30 mg/ml ΔCT694
- 30 mM NaOAc, pH 4.5
- 0.9 M NaCl

Unfortunately, overall over the course of this optimisation, the granular precipitate improved only very slightly into a microcrystalline precipitate, which can be seen in Figures 37 and 38.

4.3 - PmpD F2 characterisation experiments

A number of relatively simple characterisation experiments were performed, using SDS-PAGE and native gel analysis to monitor the behaviour of PmpD F2 under certain conditions.

The reducing agent native gel experiment result (Figures 39 and 40) appeared to show the opposite of what was expected. The aim was to determine if using reducing agents could be a method of producing a higher ratio of monomeric to oligomeric protein. It was predicted that reducing agents would cause intermolecular disulfide bonds to break or not be formed, and therefore increase the monodispersity of the PmpD F2 and allow it to flow through the gel more readily, but this was not the case. It was theorised that intramolecular disulfide bonds were interfered with, causing the PmpD F2 molecules to become unstable and aggregate with one another. As a result of this experiment, adding reducing agent to purification buffers was ruled out for PmpD F2.

The SDS-PAGE pH gradient experiment result (Figures 41 and 42) was somewhat disappointing. The interest here was to determine if a certain pH altered the state or induced cleavage of PmpD, giving some information as to how it functions in the context of *C. trachomatis* infection. As mentioned before (see page 11), PmpD undergoes some cleavage once present in the cytosol of the host cell[29]. If this cleavage was induced by a change in pH, breakdown of PmpD F2 at some point in the pH range of this experiment would corroborate with this. However, it seems that pH change alone does not affect PmpD in this way. This led on to the protease experiments.

The protease experiments (Figures 43 to 45) would have been explored more extensively given more time with the project. Upon the negative result of the pH gradient gel, digesting the protein with various proteases and determining what fragments were produced were the logical next steps. This experiment was attempted in order to ascertain the scale of timepoints and protease concentrations necessary for further experiments. The long-term plan was to optimise the experiment to give useful information about the nature of PmpD F2's immediate fragments. If fragments were seen which appeared to be a similar molecular weight of those recorded in other studies, the protein bands would be cut out of the SDS-PAGE gel and sent for analysis by mass spectrometry to confirm that they are the same. Evidence about which proteases can produce which fragments would be interesting with respect to understanding how these fragments are formed in the host cell cytosol.

5.0 - Future work

5.1 - ΔCT694 + CT166

Given more time with this project, there are multiple aspects which could be expanded and investigated more thoroughly. Crystallisation and stability studies would be continued on ΔCT694, and began on CT166. For ΔCT694, other variables and conditions to try include cleavage of the His-tag to determine if this affects protein crystallisation suitability, as well as the usage of Thermafluor assays testing many buffer conditions for improvements in protein stability, including detergent buffers. Taking the buffer conditions with the lowest protein melting temperature could provide us with another starting point for crystallisation optimisation, by modifying and adding reagents to the buffers which keep ΔCT694 the most stable and taking forward any improvements in crystal stage.

Buffer optimisation with the help of the Thermafluor technique would be a good idea with CT166, as the purification process produced a low net yield of soluble protein (Figure 29) when compared to that of ΔCT694 and PmpD F2 according to purification gels (Figures 20 and 33 for respective examples). Using a buffer which stabilises the protein more may increase the yield by decreasing the amount which is lost by aggregation. Other expression systems may also be tested to see if the gross yield of protein from the bacterial cells could increase. Upon increasing the amount of CT166 produced, the crystallisation strategy for CT166 would depend on the results of the Thermafluor assay and also what works well for ΔCT694; if there are multiple buffers in which CT166 is relatively stable, these could be experimented with as custom crystallisation screens, and if certain conditions are promising for ΔCT694, they may well be for CT166 as well bearing in mind they are thought to act in similar environments in the context of *C. trachomatis* infection.

Overall this work has laid foundations for studying these two proteins in more detail. The knowledge gained about handling these proteins, as well as the materials produced such as cloned DNA and crystal screens, will be very useful within the group as work continues towards the main goal of obtaining X-ray crystal structures for ΔCT694 and CT166.

5.2 - PmpD

Work on PmpD fragments F1, F3 and F4 halted at the gene cloning stage; not much time was put into them due to other subprojects taking priority, mainly ΔCT694 crystallisation. If this project were to be continued, all three fragments would be worked on to eventually produce high-quality protein, in order to compare their properties to each other and to those of PmpD F2 through characterisation experiments such as protease screens. Also, crystallisation trials would be tried on both the oligomer and monomer of all four fragments extensively, given that they are all slightly different to one another but solving the structure of only one of them would give much-desired insight into the function and intricacies of the PmpD protein.

The buffers used when purifying PmpD F2 could be optimised; given that it is a membrane protein with a hydrophobic region and the main buffer used when purifying is the same as ΔCT694, it seems likely that using or adding other reagents (for example, detergents) may keep the protein more stable during production. The use of Thermafluor would help with finding the optimal buffer. Finally, the protease screen tried towards the end of the project requires some optimisation steps as well before it can be useful. Once it the concentration of protease, incubation time etc. are at appropriate levels to determine the primary breaks in the protein chain, the fragments generated in the gel could be cut out and sent for mass spectrometry analysis.

The experience gained within the group of synthesising and handling PmpD F2 will be very useful as vaccine studies continue and interest in this protein as a therapeutic target continues to grow. There is also opportunity for optimisation of purification to acquire very high-quality protein, and focussing on preparing PmpD fragments for X-ray crystallisation in the future.

References

1. Omsland et al, 2012. “Developmental stage specific metabolic and transcriptional activity of *Chlamydia trachomatis* in an axenic medium.” Proc Natl Acad Sci USA **109** 19781-85
2. Eissenberg et al, 1983. “Chlamydia psittaci elementary body envelopes: ingestion and inhibition of phagolysosome fusion.” Infect Immun **40** (2) 741-751
3. Hackstadt et al, 1995. “Lipid metabolism in *Chlamydia trachomatis*-infected cells: directed trafficking of Golgi-derived sphingolipids to the Chlamydial inclusion.” Proc Natl Acad Sci USA **92** 4877-881
4. Carabeo R, 2011. “Bacterial subversion of host actin dynamics at the plasma membrane.” Cell Microbiol **13** (10) 1460-1469
5. Chi et al, 1987. “Unique ultrastructure in the elementary body of Chlamydia sp. strain TWAR”. J Bacteriol **169** (8) 3757-3763
6. Clifton et al, 2004. “A Chlamydial type III translocated protein is tyrosine-phosphorylated at the site of entry and associated with recruitment of actin.” Proc Natl Acad Sci USA **101** 10166-171
7. Brinkworth et al, 2011. “*Chlamydia trachomatis* Slc1 is a type III secretion chaperone that enhances the translocation of its invasion effector substrate TARP.” Mol Microbiol **82** 131-144
8. Jewett et al, 2006. “Chlamydial TARP is a bacterial nucleator of actin.” Proc Natl Acad Sci USA **103** 15599-15604
9. Jiwani et al, 2012. “*Chlamydia trachomatis* Tarp cooperates with the Arp2/3 complex to increase the rate of actin polymerisation.” Biochem Bioph Res Co **420** 816-821
10. Derre et al, 2011. “The lipid transfer protein CERT interacts with the Chlamydia inclusion protein IncD and participates to ER-Chlamydia inclusion membrane contact sites.” PLOS Pathog **7** e1002092
11. Suchland et al, 2000. “Isolates of *Chlamydia trachomatis* that occupy nonfusogenic inclusions lack IncA, a protein localized to the inclusion membrane.” Infect Immun **68** 360-367
12. World Health Organisation, 2014. “Trachoma Fact Sheet №382”. www.who.int/mediacentre/factsheets/fs382/en
13. Fenwick, A, 2008. “The global burden of neglected tropical diseases”. Public Health **126** (3) 233-236
14. Burton, M and Mabey D, 2009. “The global burden of trachoma: a review”. PLoS Neglect Trop D **3** (10) e460

15. International Trachoma Initiative, 2012. “WASH: Water, Sanitation and Hygeine”. www.trachoma.org/index.php?q=core/sub.phpandcat=trachomaandid=trachoma
16. CDC Grand Rounds, 2011. “Chlamydia prevention: challenges and strategies for reducing disease burden and sequelae.” Morbidity and Mortality Weekly Report **60** (April (12)) 370-373
17. World Health Organisation, 2001. “Global prevalence and incidence of selected curable sexually transmitted infections: overview and estimates.” www.who.int/hiv/pub/sti/who_hiv_aids_2001.02.pdf
18. Vos, T, 2012. "Years lived with disability (YLDs) for 1160 sequelae of 289 diseases and injuries 1990-2010: a systematic analysis for the Global Burden of Disease Study 2010”. Lancet **380** (9859) 2163-2196
19. Lozano, R, 2012. “Global and regional mortality from 235 causes of death for 20 age groups in 1990 and 2010: a systematic analysis for the Global Burden of Disease Study 2010”. Lancet **380** (9859) 2095-128
20. Brunham RC and Rekart ML, 2009. “Considerations of *Chlamydia trachomatis* disease expression.” FEMS Immunol Med Mic **55** (March (2)) 162-166
21. Brunham RC and Rekart ML, 2008. “The arrested immunity hypothesis and the epidemiology of Chlamydia control.” Sex Transm Dis **35** (January (1)) 53-54
22. Brunham RC and Rappuoli R, 2013. “*Chlamydia trachomatis* control requires a vaccine.” Vaccine **31** 1892-97
23. Li Z and Dai W, 2014. “Conserved type III secretion system exerts important roles in *Chlamydia trachomatis*.” Int J Clin Exp Pathol **7** (9) 5404-5414
24. Hower et al, 2009. “Evidence that CT694 is a novel *Chlamydia trachomatis* T3S substrate capable of functioning during invasion or early cycle development.” Mol Microbiol **72** (6) 1423-1437
25. Bullock et al, 2012. “Domain analyses reveal that *Chlamydia trachomatis* CT694 protein belongs to the membrane-localised family of type III effector proteins.” J Biol Chem **287** 28078-86
26. Coldwell J, 2014. “Characterisation of putative early effectors of *Chlamydia trachomatis* infection.” (BSc project report)
27. Thalmann et al, 2010. “Actin re-organization induced by *Chlamydia trachomatis* serovar D – evidence for a critical role of the effector protein CT166 targeting Rac.” PLOS ONE **5** (3) e9887
28. Bothe et al, 2015. “DXD motif-dependent and –independent effects of the *Chlamydia trachomatis* cytotoxin CT166.” Toxins **7** 621-637

29. Swanson et al, 2009. "*Chlamydia trachomatis* polymorphic membrane protein D is an oligomeric autotransporter with a higher-order structure". Infect Immun **77** (1) 508-516
30. Kiselev et al, 2009. "Analysis of pmpD expression and PmpD post-translational processing during the life cycle of *Chlamydia trachomatis* serovars A, D, and L2." PLOS ONE **4** (4) e5191
31. Crane et al, 2005. "*Chlamydia trachomatis* polymorphic membrane protein D is a species-common pan-neutralizing antigen." Proc Natl Acad Sci USA **103** (6) 1894-1899
32. IonSource LLC, 2016. http://www.ionsource.com/Card/cmc/cmc.htm